An Acad Bras Cienc (2025) 97(Suppl. 1): e20240478 DOI 10.1590/0001-3765202520240478
Anais da Academia Brasileira de Ciências | *Annals of the Brazilian Academy of Sciences*
Printed ISSN 0001-3765 I Online ISSN 1678-2690
www.scielo.br/aabc | www.fb.com/aabcjournal

PALEONTOLOGY

Flesh and bone: The musculature and cervical movements of pterosaurs

RICHARD BUCHMANN & TAISSA RODRIGUES

Abstract: The osteological variations present in the cervical vertebrae of pterosaurs represent changes in the soft tissues of the neck and reflect their function. Here, we infer the presence, volume, and capacity of the cervical musculature of pterosaurs. We performed our analyses on three-dimensionally preserved cervical series of *Anhanguera* sp. (AMNH 22555), *Anhanguera piscator* (NSM-PV 19892), *Azhdarcho lancicollis* (ZIN PH and CCMGE, several specimens), and *Rhamphorhynchus muensteri* (MGUH 1891.738), the last three of which were digitally modeled for muscle reconstruction. We identified osteological correlates from structures observed in extant archosaur vertebrae and skulls and supported by Extant Phylogenetic Bracket (EPB) criteria. We estimated the muscular capacity using the "Maximal Force Production" formula. According to our analyses, at least thirteen muscles were present in the neck of pterosaurs, only one of which does not correspond to an EPB level I inference. The muscles that performed skull and neck pitching were more robust and stronger to execute the movements. Muscles that showed extremely low potential had a more cervical stabilization function. Specializations we identified in the muscles are compatible with the foraging habits previously inferred for these pterosaurs, namely surface fishing by *Rhamphorhynchus* and *Anhanguera* and capture of small terrestrial prey by *Azhdarcho*.

Key words: Archosauria, cervical biomechanics, cervical muscles, cervical vertebrae, neck, Pterosauria.

INTRODUCTION

Pterosaur cervical vertebrae had unique specializations, varying morphologically between species and in different areas of the neck within the same individual (Wellnhofer 1991a, Kellner & Tomida 2000, Bennett 2001, Veldmeijer et al. 2009, Eck et al. 2011, Vila Nova et al. 2015, Buchmann et al. 2018, Andres & Langston Jr. 2021). Usually, their neck was anatomically segmented in the anterior cervical vertebrae (atlas and axis), the mid-cervical vertebrae (third to seventh), and the posterior cervical vertebrae (eighth and ninth) (Bennett 2001, Vila Nova et al. 2015). The anatomical complexities of these different segments reflected variations in the attachments of soft tissues, such as joints, ligaments, and muscles (Tambussi et al. 2012, Cobley et al. 2013). Muscle attachment sites in pterosaur vertebrae can be recognized through osteological correlates in extant archosaurs, and these inferences can be supported based on the criteria of the Extant Phylogenetic Bracket method of inference (Witmer 1995).

Inferences of well-developed cervical musculature in pterosaurs have previously been made, mainly by the identification of robust insertion sites in the occipital region of the skull of *Rhamphorhynchus muensteri*, *Anhanguera*, *Dsungaripterus weii*, and azhdarchids (Witmer et al. 2003, Habib & Godfrey 2010, Naish & Witton 2017). Dorsal muscles arranged superficially at the base of the neck and associated with the

execution of appendicular movements were also previously inferred in *Pteranodon*, *Barbosania*, and *Quetzalcoatlus* (Bennett 2003, Elgin & Frey 2011, Padian et al. 2021). However, a complete analysis identifying possible osteological correlates in cervical vertebrae of different pterosaurs has not yet been performed.

Furthermore, inferences about pterosaur foraging habits and locomotion have often been presented disregarding the activity of the cervical muscles (Nesov 1984, Kellner & Langston Jr. 1996, Prieto 1998, Kellner & Tomida 2000, Kellner & Campos 2002, Humphries et al. 2007, Averianov 2013, Padian et al. 2021, Williams et al. 2021). The procoelous condyles of the cervical vertebrae indicate that the long necks of pterosaurs were mobile (Bennett 2001, Fronimos & Wilson 2017), but the convexity of the condyles and the length of the vertebral processes, especially in Pteranodontoidea, indicate that the neck was not as sinuous and flexible as that of extant birds (Boas 1929, Zusi 1962, Kellner & Tomida 2000, Bennett 2001, Guinard et al. 2010, Muller et al. 2010, Eck et al. 2011, Cobley et al. 2013, Vila Nova et al. 2015, Fronimos & Wilson 2017, Buchmann et al. 2018, Terray et al. 2020, Andres & Langston Jr. 2021). The identification of sites of insertion and inferences of muscle volume can more assertively demonstrate relative efficiencies of pterosaur muscles for specific actions, and allow to extrapolate the cervical movements performed by pterosaurs (Boumans et al. 2015, Porro et al. 2011).

Here, we aim to identify the muscles of the cervical vertebrae and occipital region of pterosaurs and compare the performance of each of them.

MATERIALS AND METHODS

To infer pterosaur cervical muscles, we analyzed the cervical vertebrae of a referred specimen of *Rhamphorhynchus muensteri* (MGUH 1891.738), a non-pterodactyloid pterosaur housed in the Geological Museum/Natural History Museum of Denmark, Copenhagen, Denmark (Bonde & Christiansen 2003); among pterodactyloids, a specimen attributed to *Anhanguera* sp. (AMNH 22555), housed at the American Museum of Natural History, New York, USA (Wellnhofer 1991b, Pinheiro & Rodrigues 2017); the holotype of *Anhanguera piscator* (NSM-PV 19892), housed in the collection of the National Museum of Nature and Science, in Tsukuba, Japan (Kellner & Tomida 2000); and of several specimens of *Azhdarcho lancicollis*, housed in the Paleoherpetological collection of the Zoological Institute of the Russian Academy of Sciences (ZIN PH; several specimens) and in the Chernyshev's Central Museum of Geological Exploration (CCMGE 1/11915 and 7/11915), both in Saint Petersburg, Russia (Averianov 2010). We chose these specimens for the excellent three-dimensional preservation of almost all vertebrae, which enabled the recognition of osteological correlates. To reconstruct the cervical muscles, we produced 3D digital models of the cervical vertebrae of the above-mentioned specimens. Computed tomography scans of the *Anhanguera piscator* holotype were obtained at 300 to 310 kV and 200 µA, with voxel sizes ranging from 0.065 to 0.175. The plate containing *Rhamphorhynchus muensteri* (MGUH 1891.738) was scanned at 120 kV and 280 µA, with voxel sizes of 0.2 mm. Specimens belonging to *Azhdarcho lancicollis* (ZIN PH; several specimens and CCMGE 1/11915 and 7/11915) were scanned by non-contact 3D laser and provided for this research by Alexander Averianov (Zoological Institute of the Russian Academy of Sciences, Russia) (see Buchmann & Rodrigues 2024a for more details on obtaining data and generating the three-dimensional models). AMNH 22555 was not digitized due to the anatomical similarity of the locations

of the muscular attachments of the cervical vertebrae with *Anhanguera piscator*, which demonstrates that both had an anatomically similar arrangement of the cervical muscles. The digitized cervical series were reconstructed and articulated and are available on Morphosource (Boyer et al. 2017) under the following DOI: 10.17602/M2/M588059 (*Rhamphorhynchus muensteri*; Media ID 000588059), 10.17602/M2/M589271 (*Anhanguera piscator*; Media ID 000589271) and 10.17602/M2/M59913 (*Azhdarcho lancicollis*; Media ID 000599131) (Buchmann & Rodrigues 2024a).

The inferred cervical musculature was supported by the Extant Phylogenetic Bracket (EPB), which defines criteria for the level of soft tissue inferences based on the osteological correlates presented by extant specimens from groups phylogenetically close to the extinct study group (Witmer 1995). Levels of inference I, II, and III are established when the osteological correlate that determines the presence of soft tissue is present in the extinct group and in both extant groups, only in one of the extant groups, or in none of the extant groups, respectively (Witmer 1995). The variation of inference levels I', II', and III' are used when osteological correlates are absent in the extinct group (Witmer 1995). We followed the hypothesis of homology between extant bird and crocodylian neck muscles established by Tsuihiji (2005, 2007). The names suggested for the musculature of pterosaurs were based on the greatest similarity between the locations, amount, and shape of attachments of the muscles of extant birds or crocodylians.

To represent extant outgroups in the EPB, we dissected avian and crocodylian specimens. To recognize the locations of muscular attachments in extant birds, we dissected eleven Phaethoquornithes (*Ardea alba*, *Calonectris diomedea*, *Fregata magnificens*, *Ixobrychus exilis*, *Nannopterum brasiliensis*, *Phaeton aethereus*, *Procellaria aequinoctialis*, *Puffinus puffinus*, *Sula leucogaster*, *Thalassarche chlororhynchos* and *Thalassarche melanophris*, four Charadriiformes (*Haematopus palliates*, *Larus dominicanus*, *Sterna hirundo*, and *Thalasseus acuflavidus*), and two Telluraves (*Coragyps atratus* and *Cariama cristata*) (sensu Kuhl et al. 2021, Braun & Kimball 2021). We chose to analyze Phaethoquornithes and Charadriiformes due to their diverse aquatic foraging habits, which resemble those inferred for *Rhamphorhynchus muensteri* and *Anhanguera* (Wellnhofer 1975, Sick 1997, Schreiber & Burger 2001, Phalan et al. 2007, Amiot et al. 2010, Tütken & Hone 2010, Frey & Tischlinger 2012, Veldmeijer et al. 2012, Wang et al. 2012, Hone et al. 2013, Weimerskirch et al. 2013, Bestwick et al. 2018, Gheler-Costa et al. 2018, Pêgas et al. 2020). The choices of *Coragyps atratus* and *Cariama cristata* were based on their more terrestrial habits, which are inferred for *Azhdarcho lancicollis* (Kruuk 1967, Redford & Peters 1986, Houston 1988, Witton & Naish 2008, 2015, Bestwick et al. 2018). To recognize the locations of muscular attachments in crocodylians, we dissected a specimen of *Caiman latirostris*. The birds and *Caiman latirostris* dissected during this study were euthanized after veterinary treatment at the Instituto de Pesquisa e Reabilitação de Animais Marinhos (IPRAM, in Cariacica, ES, Brazil) (under authorizations SISFAUNA IEMA 001/2014, process 68077610; IEMA 001/2014, process 67277780; and SISBIO 34510 and 26896) and Projeto Caiman (Instituto Marcos Daniel, in Vitória, ES, Brazil) (under authorization SISBIO 92997549), respectively. Anatomical nomenclature that had not yet been used for pterosaur vertebrae followed the *Nomina Anatomica Avium* (Baumel & Witmer 1993).

We took measurements of extant birds to observe the proportion between the space filled

by bone and muscle along the neck at different stages of dissection: the width and height of the neck were measured in the musculature surrounding the vertebrae using a caliper before we began the dissection; the thickness of the muscle bundles were measured at the sites of origin and mid-length using measuring tape during dissection; and the maximum width of the cervical vertebrae was measured by caliper after all soft tissues had been removed. We decided to analyze this ratio only in birds due to the anatomical similarity of avian and pterosaur cervical vertebrae, which present short processes and reduced ribs, when present (Buchmann & Rodrigues 2024a).

We made the muscle arrangement reconstruction and volume quantification using Blender 3D software, version 4.0 (Blender Development Team 2019). The deep contour of the musculature was defined according to the shape of the cortex of the cervical vertebrae of pterosaurs. The muscles were reconstructed from cylinders, whose bases area was equivalent to 0.2 cm^2. The position of the muscle in relation to the vertebra was defined after identifying the sites of muscle attachments in extant archosaurs and recognizing osteological correlates in pterosaur vertebrae. Subsequently, the path taken by the muscle bundles was defined using the OpenSim software, version 4.4, in which we used "wrapping surfaces" to guide the bundles along the joints (Hutchinson et al. 2005, 2008, Delp et al. 2007, Bates & Schachner 2012). The cylinders representing each muscle were positioned parallel to the cervical vertebrae, and their bases were dimensioned following the thickness pattern observed in cervical muscles of extant birds (see results in "Volume and Maximum Force Production (F_{pmax}) of the muscles"). The increased thickness of the cylinders turned them into free-form meshes, the contact between which was defined through the path taken by the muscle bundles and pre-established thickness according to the pattern seen in extant birds. The external contours of the cervical musculature were defined using 32-sided polygonal hoops, which were positioned around each cervical vertebra, except the atlas (Allen et al. 2009). The size of the polygonal hoops was defined according to the proportion observed between the width of the vertebrae and the outer edge of the musculature of the analyzed extant birds (see results in "Volume and Maximum Force Production (F_{pmax}) of the muscles"). When the increase in the thickness of the superficially arranged meshes was limited by the polygonal hoops, we modeled them to fill the empty spaces in the cross-section until reaching the pre-established area for the muscle thickness. After delimiting the thickness of each muscle within the polygonal hoops, we interconnected the edges of each mesh with the adjacent one, which finalized the three-dimensional model of the muscles. The meshes that represented segmented muscles were properly closed, without connection to the adjacent one. Finally, we subjected the three-dimensional muscles to the volume calculation using the 3D printing extension of Blender 3D software, version 4.0 (Blender Development Team 2019). We quantified muscle capacity using "Maximal Force Production" (F_{pmax}), which is widely recommended for estimating muscle strength in extinct animals (Porro et al. 2011, Bishop et al. 2021). The maximum force exerted by muscles is produced during isometric contractions and is expressed by Equation 1:

$$F_{pmax} = \frac{m_{musc}.\sigma.\cos(\alpha o)}{\rho.\ell o} \quad (1)$$

Where m_{musc} is the muscle mass, σ is the maximum tension developed in the muscle fibers, $\cos(\alpha o)$ is the cosine of the pennation

angle at fiber length, ρ is the density of the muscle tissue and ℓo is the optimum muscle bundle length (Porro et al. 2011, Bishop et al. 2021). To calculate muscle mass (m_{musc}), we applied the constant density of 1000 kg m^3 in the reconstructed muscles, as indicated for archosaur soft tissues (Allen et al. 2009, Macaulay et al. 2017). We considered the $\cos(\alpha o)$ value only for the calculation of the *splenius capitis*, since the pennation is parallel to the fibers in the other cervical muscles of extant archosaurs (Cox et al. 2019). The σ and ρ parameters were set at 300,000 N/m^2 and 1060 kg/m^3, as generally used for vertebrate skeletal muscles (Hutchinson et al. 2015). To take into account the constraints on the path of the muscle bundles, we used the "wrapping surfaces" and measured their length (ℓo) in OpenSim software, version 4.4 (Hutchinson et al. 2005, 2008, Delp et al. 2007, Bates & Schachner 2012, Bishop et al. 2021).

Anatomical abbreviations

ac, *ansa costotransversaria*; asc, *ascendens cervicalis*; atr, atlas rib; ax, axis; axr, axis rib; bast, *basal tubera*; biv, *biventer cervicis*; bo, basioccipital; ca, *capitulum*; cat, *capitulum* of the atlas; cax, *capitulum* of the axis; cnt, *crista nuchalis transversa*; com, *complexus*; cop, costal process; cr, cervical rib; epi, epipophysis; fcl, *flexor colli lateralis*; fco, *flexor colli*; fm, *foramen magnum*; fopn, pneumatic fomanen; hyp, hypapophysis; icr, *intercristales*; ilca, *iliocostalis capitis*; ilce, *iliocostalis cervicis*; isp, *interspinales*; itr, *intertransversarii*; lcs, *longissimus capitis superficialis*; lce, *longissimus cervicis*; lcp, *longissimus capitis profundus*; lco, *longus colli*; lcv, *longus colli ventralis*; ldca, *longus colli dorsalis*, *pars caudalis*; mus, muscle scar; nc, neural canal; ns, neural spine; oc, occipital condyle; poex, postexapophysis; prex, preexapophysis; pp, paraoccipital process; poz, postzygapophysis; pra, proatlas; prz, prezygapophysis; ptf, posttemporal fenestra; rcam, *rectus capitis anticus major*; rcd, *rectus capitis dorsalis*; rcl, *rectus capitis lateralis*; rcv, *rectus capitis ventralis*; sca, *scalenus*; sk, skull; soccr, supraoccipital crest; spc, *splenius capitis*; ta, *tuberculum ansae*; tat, atlas tubercle; tax, axis tubercle; tca, *transversospinalis capitis*; tce, *transversospinalis cervicis*; td, *torus dorsalis*; toc, transverse oblique crest; trp, transverse process; tub, tubercle; vf, *vagus foramen*; vp, ventral process.

Muscle attachment sites and thickness in extant archosaurs

The anatomy of the cervical vertebrae of both extant archosaur clades varies along the neck, which consequently alters the shape and extent of the sites of muscular attachments in the vertebral cortex. The dorsal surface of the atlas is prominent in both extant archosaurs and is associated with the *epistropheo-capitis* and *atloïdo-capitis* in *Caiman latirostris* and the *splenius capitis* in birds (Figure 1). In the neural arch of the atlas of both those clades, the muscles are attached to two pairs of lateral tubercles that have well-defined muscle scars and rough edges (Figure 1). These tubercles are attachment sites for the *longissimus capitis profundus* and *longissimus cervicis* in *Caiman latirostris* and the *rectus capitis dorsalis* in birds. Their atlas has ventral extensions: the hypapophysis in birds and the ventral process in *Caiman latirostris* (Figure 1). Both structures have rough lateral and medial surfaces and are sites of muscular attachments of the *rectus capitis anticus major* and *longus colli* in *Caiman latirostris* and of the *rectus capitis lateralis*, *rectus capitis ventralis*, and *longus colli ventralis* in extant birds.

The cranial surface of the neural spine of the axis of *Caiman latirostris* and birds has a well-developed muscle scar, which is the site of

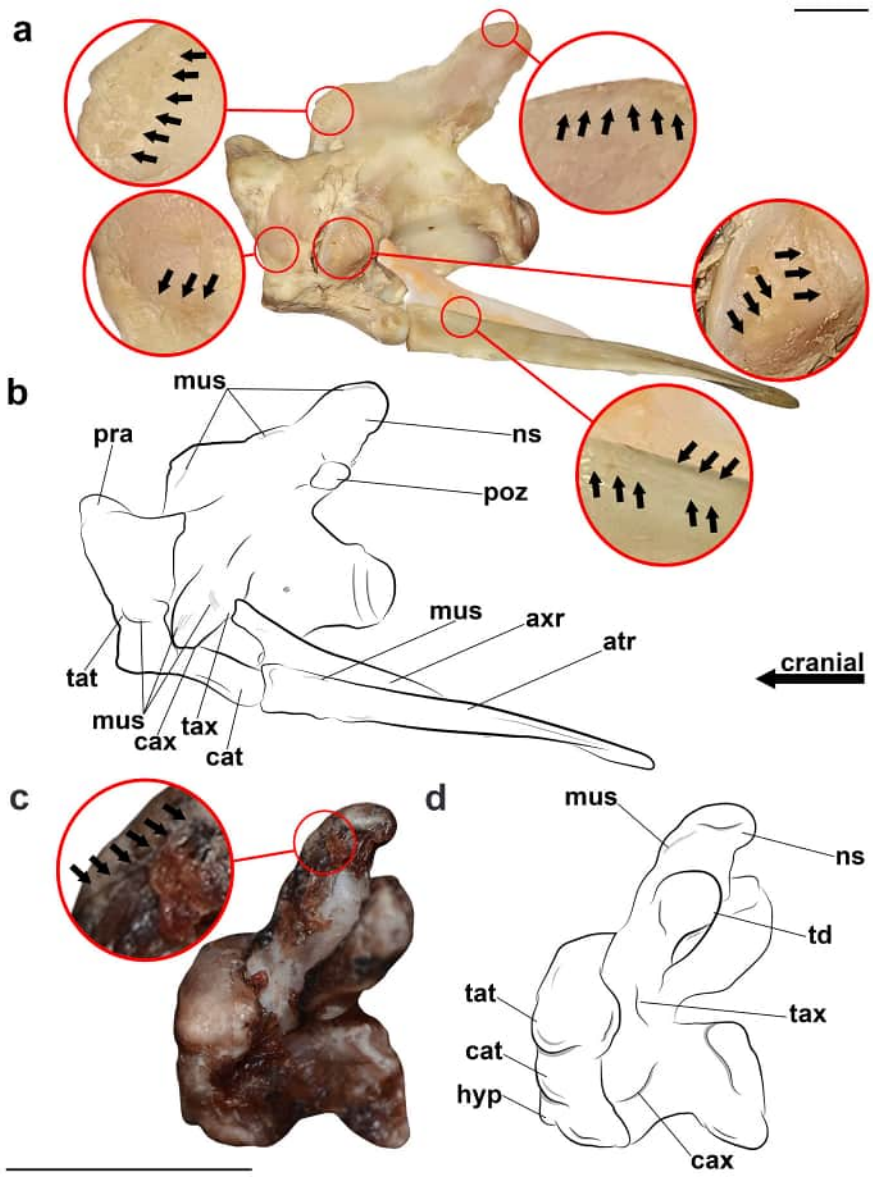

Figure 1. Photographs and interpretative drawings of the atlas and axis in left lateral view of *Caiman latirostris* (a, b) and *Procellaria aequinoctialis* (c, d). Arrows indicate muscle scars. Scale bar: 10 mm.

attachment of the *atloïdo-capitis* and *splenius capitis*, respectively (Figure 1). The tall neural spines of the postaxial vertebrae of *Caiman latirostris* present rough areas and muscle scars on the top and on the cranial and caudal sides, which are associated with *transversospinalis capitis*, *spino-capitis posticus*, *transversospinalis cervicis*, *epistropheo-capitis*, and *interspinales* (Figure 2). In birds, neural spines are developed only in the cervical vertebrae located at the cranial and caudal ends of the neck, where they are attachment sites of the muscles of the *longus capitis dorsalis* group and of the *interspinales* (Figure 3).

Prominences titled *torus dorsalis* in birds and epipophyses in crocodylians have marked and rough edges in postatlantal vertebrae (Figures 1, 2 and 3). They are seen dorsally to the postzygapophyses and are sites of ligaments and of the *transversospinalis cervicis* in *Caiman latirostris* and the *longus capitis dorsalis* group in birds (Figures 1, 2 and 3). The connection between the postzygapophyses and the neural spine forms the transverse-oblique crests in

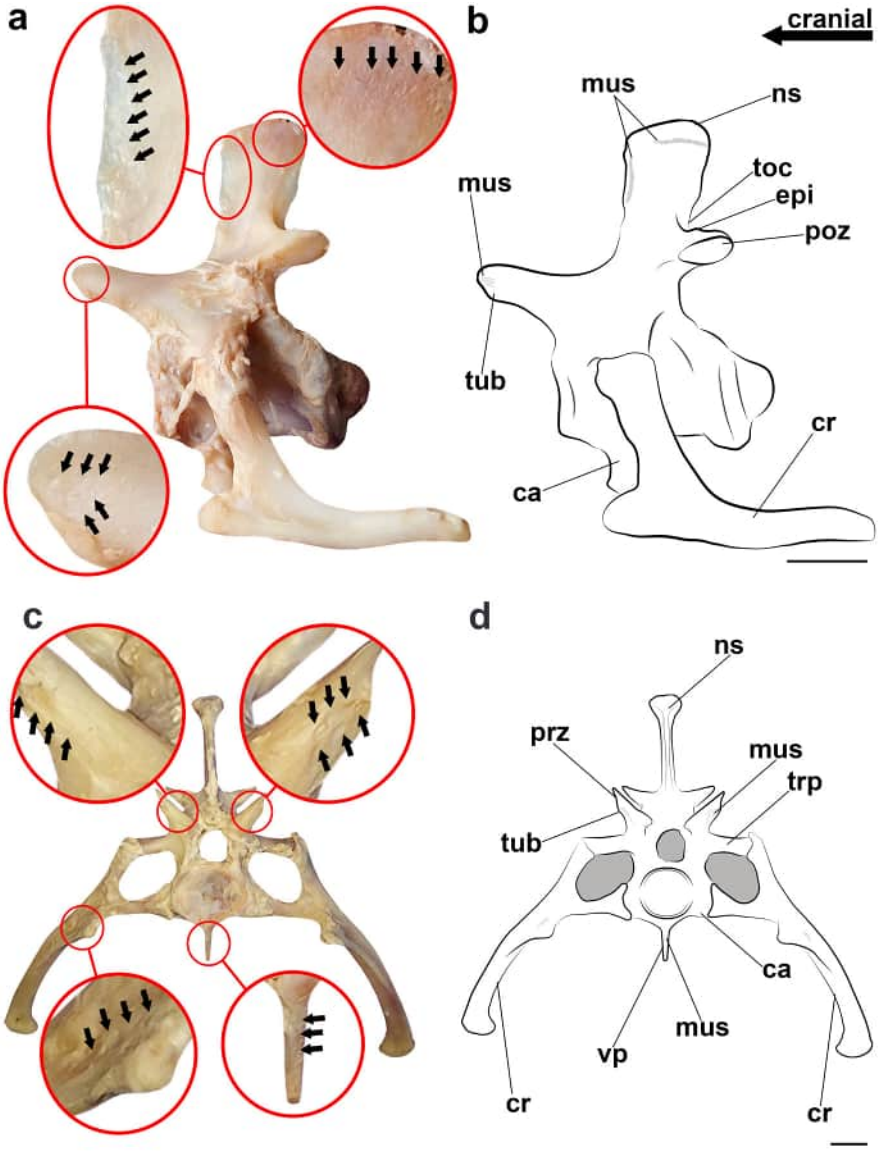

Figure 2. Photographs and interpretative drawings of the cervical vertebrae of *Caiman latirostris*. Third vertebra in left lateral view (a, b); ninth vertebra in cranial view (c, d). Arrows indicate muscle scars. Scale bar: 10 mm.

postatlantal vertebrae, which are concave and associated with segmented muscles in both these extant archosaurs (Figures 2 and 3).

Developed and very marked tubercles arranged laterally on the cervical vertebrae are attachment sites of the *longissimus capitis profundus* along the entire cervical length of the neck of *Caiman latirostris* (Figures 1 and 2). In the *ansa costotransversaria* of the cervical vertebrae of birds, there are a pair of *tubercula ansae* on each side of the vertebrae of the cranial and mid-segment of the neck (Figures 1 and 3). Between these structures, deep muscle scars with a rough surface are observed, which are sites of attachments of the *ascendens cervicalis*, *rectus capitis dorsalis*, and *flexor colli lateralis* (Figures 1 and 3). Scars associated with the activity of these muscles border the *tuberculum ansae* of the avian vertebrae (Figure 3). Caudal to the *tuberculum ansae*, there are lateral crests with well-defined indentations that are associated with the *complexus*, *intertransversarii*, and *longus colli ventralis* attachments in birds (Figure 3). In postaxial

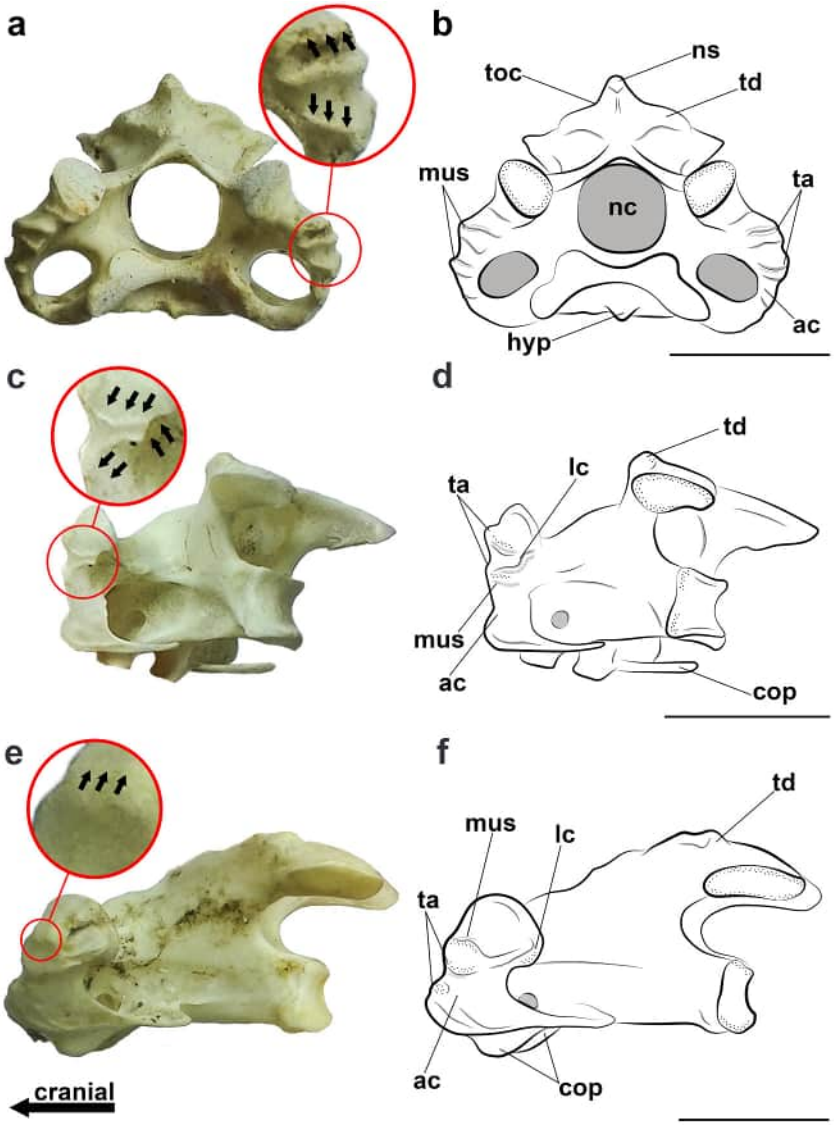

Figure 3. Photographs and interpretative drawings of the cervical vertebrae of extant birds. Fifth vertebra of *Sula leucogaster* in cranial view (a, b); eighth vertebra of *Procellaria aequinoctialis* in caudolateral view (c, d); eighth vertebra of *Fregata magnificens* in left lateral view (e, f). Arrows indicate muscle scars. Dotted regions indicate greater surface roughness. Scale bar: 10 mm.

vertebrae, the well-developed transverse processes with rough ends are also sites of muscular attachments of the *longissimus capitis superficialis*, *longissimus capitis profundus*, and *longissimus cervicis* in *Caiman latirostris* (Figure 2). This correlate is also developed in vertebrae of the caudal segment of the neck of birds, which are sites of the *intertransversarii* attachments.

In *Caiman latirostris*, the developed ventral processes along the cervical vertebrae are also the attachment sites of the *rectus capitis anticus major* and *longus colli* (Figures 1 and 2). However, in birds, the hypapophyses are developed only in the vertebrae located at the cranial and caudal ends of the neck (Figures 1 and 3). The well-developed and rough capitulum of all cervical vertebrae of *Caiman latirostris* and of the most caudal vertebrae of extant birds are also attachment sites of the *longus colli* and *longus colli ventralis*, respectively (Figure 2). Furthermore, the cervical ribs of *Caiman latirostris* and the costal processes of birds are also associated with the *iliocostalis capitis*, *iliocostalis cervicis*, *scalenus*, and *intercostales externi* and the *flexor colli lateralis*, *intertransversarii*, *inclusi*, and *longus colli*

ventralis, respectively, throughout the cervical series (Figures 1, 2 and 3).

All cervical muscles of *Caiman latirostris* have fibers parallel to the long muscular axis (Figure 4). In birds, only the *splenius capitis* and *intertransversarii* do not have fibers parallel to the long axis of the cervical muscles, which are oriented at 60° (Figure 4).

The cervical musculature of the extant birds we analyzed varies in thickness along the neck. However, the thickness along the cervical muscle bundles of birds is constant from origin to mid-length (Supplementary Material - Table SI). Therefore, the variation in muscle thickness occurs solely due to the difference in the concentration of bundles in regions along the musculature. The only exception to this pattern is the *splenius capitis*, which is short and has triangular bundles of broad insertions, a unique morphology that results in the thickest region of the muscle being near the insertions.

Despite varying thickness, the necks of extant birds exhibit a pattern of size around each cervical vertebra. We observed that the

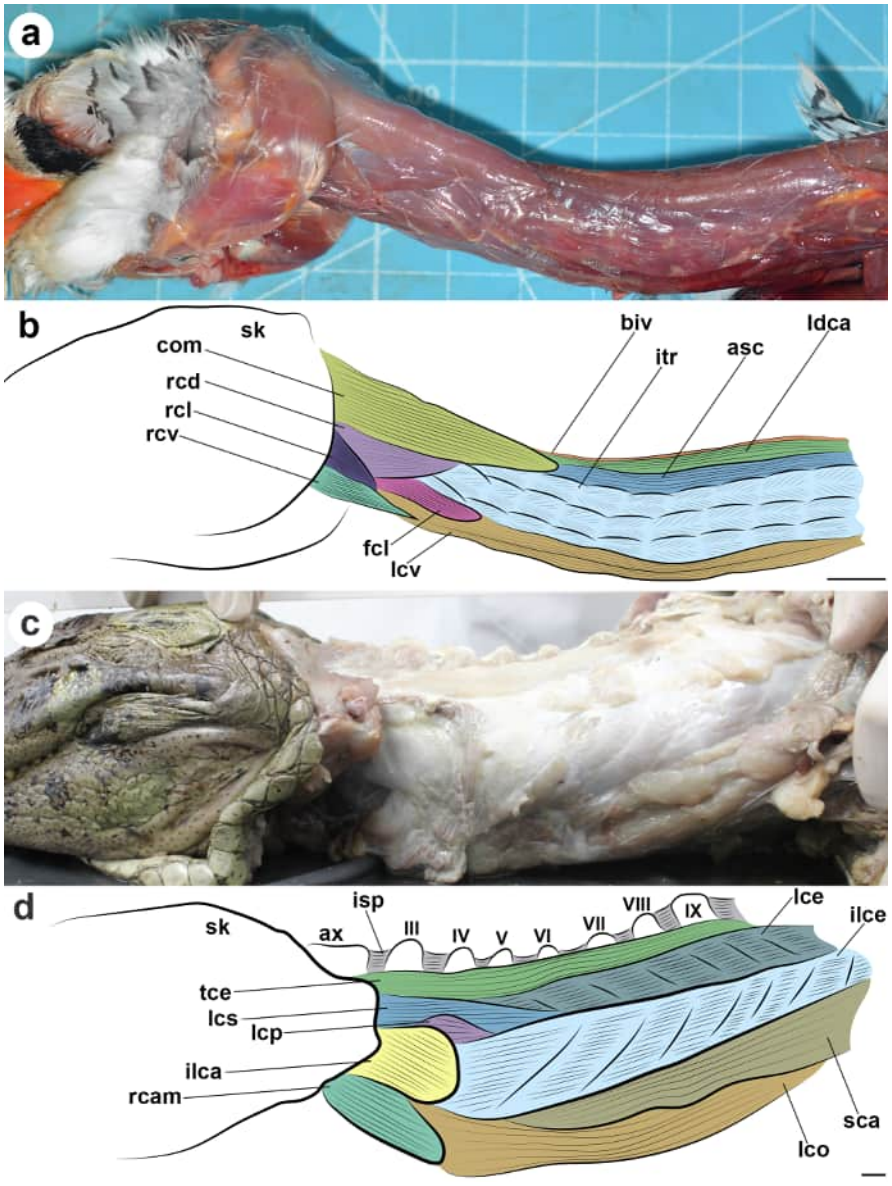

Figure 4. Photographs and interpretative drawings showing the orientation of the muscle fibers and the arrangement of the cervical muscles in extant archosaurs. Cervical musculature of *Phaeton aethereus* (a, b) and *Caiman latirostris* (c, d) in left lateral view. Roman numerals indicate the postaxial vertebrae. Scale bar: 10 mm.

width obtained between the prezygapophyses is equivalent to around two-thirds of the total width of the neck (Figure 5, Table SII). Furthermore, the width and height of the neck are approximately similar (Figure 5, Table SII).

Identification of osteological correlates in pterosaurs

The neural arches of the atlas and axis of MGUH 1891.738 (*Rhamphorhynchus muensteri*) were not preserved, which prevented us from identifying osteological correlates in this region in both vertebrae. In the pterodactyloid pterosaurs, the neural spine of the axis is tall, and its cranial surface has a well-defined muscle scar, similar to the scar observed in *Caiman latirostris* and birds (Figures 1 and 6). The neural spines of the postaxial vertebrae are tall throughout the cervical series in *Anhanguera* and *Rhamphorhynchus muensteri*, which are observed in the latter's counter slab (Figure 7). The cervical vertebrae of *Azhdarcho lancicollis* have reduced neural spines in the mid-cervical vertebrae. In *Anhanguera*, the posterior cervical vertebrae have tall neural spines with a blade-like

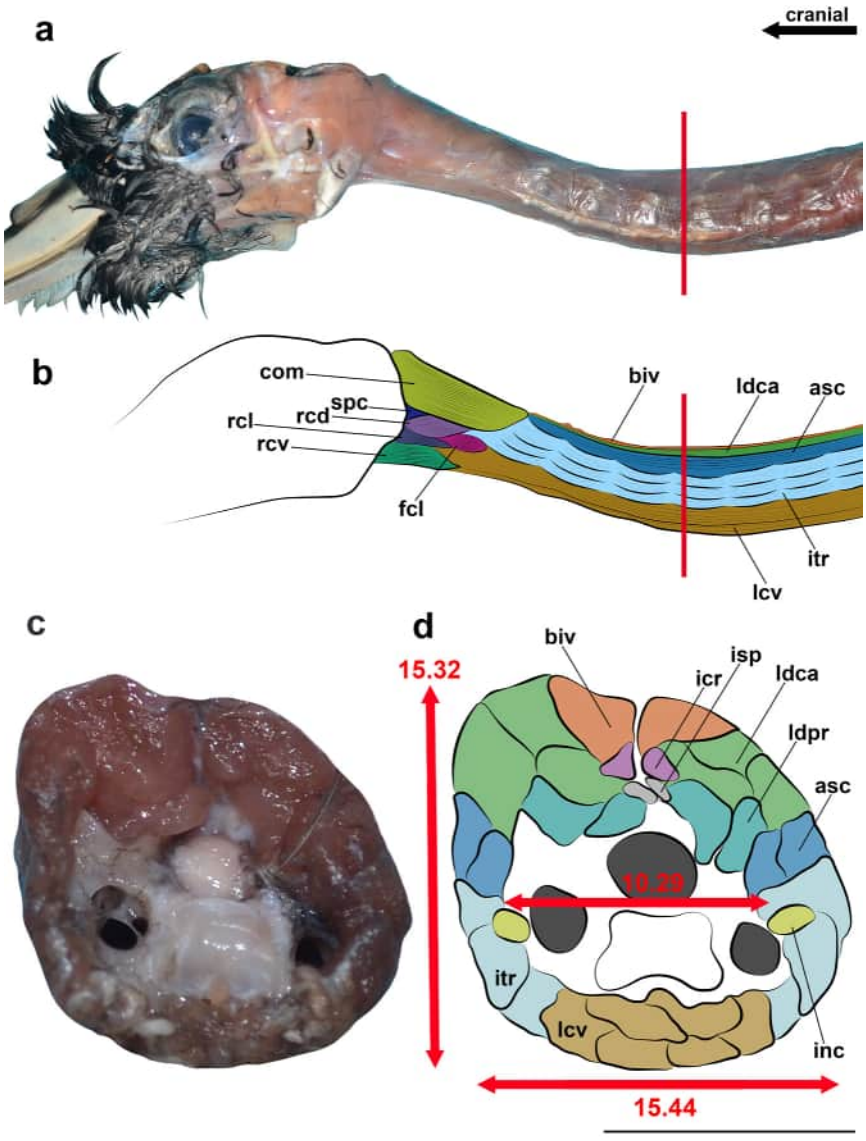

Figure 5. Scheme showing the arrangement and proportion of the musculature in relation to the space occupied by the vertebra in the neck of *Procellaria aequinoctiallis*. Photograph and interpretive drawing of the neck in left lateral view (a, b); Photograph and interpretive drawing of the cross section showing the cranial view of the ninth cervical vertebra (c, d). Red bar (a, b) indicates the location of the cross section shown. Red arrows (d) indicate the collected measurements. Measurements (d) are shown in millimeters. Scale bar: 10 mm.

shape, differing from the spike-like shape of its mid-cervical vertebrae (Figures 7 and 8). The shape of the neural spines of *Rhamphorhynchus muensteri* does not vary along the neck, and the analyzed material of *Azhdarcho lancicollis* does not present this structure preserved in posterior vertebrae. The neural spines of all cervical vertebrae are rough and have well-defined muscle scars, as in *Caiman latirostris* (Figures 1, 2, 7 and 8). Subtle muscular scars are seen on the cranial and caudal aspects of the neural spine of the cervical vertebrae of *Anhanguera* sp. (AMNH 22555) (Figure 7).

Robust epipophyses are present on the dorsal surface of the postzygapophyses of *Anhanguera* and *Azhdarcho lancicollis*, as seen on the *torus dorsalis* and epipophyses of extant birds and *Caiman latirostris*, respectively (Figures 1, 2, 3, 6, 7 and 8). The epipophyses of the axis and the eighth vertebra are the most developed of all in the cervical series, while in the ninth vertebra they are more discrete (Figures 6, 7 and 8). There is a well-defined and

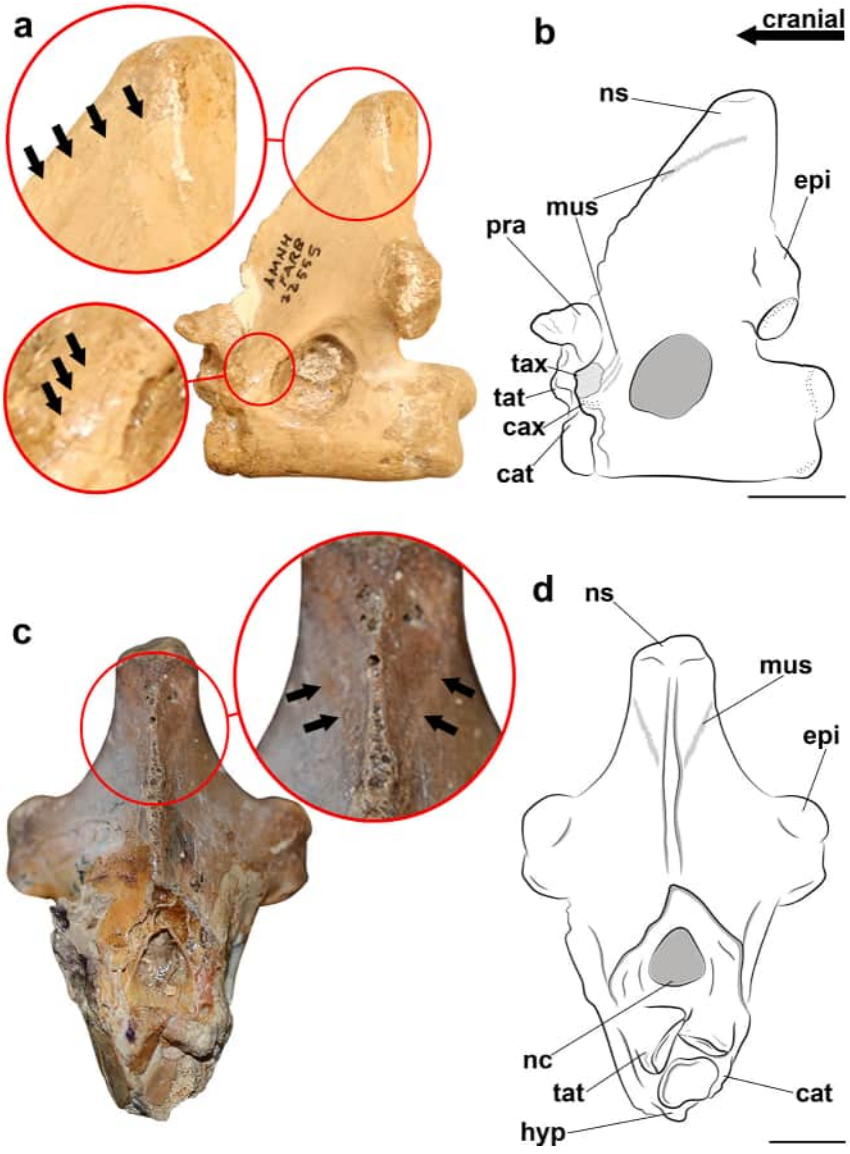

Figure 6. Photographs and interpretative drawings of the atlas and axis of *Anhanguera* sp. (AMNH 22555) in left lateral view (a, b) and *Anhanguera piscator* in cranial view (c, d). Arrows indicate muscle scars. Dotted regions indicate rougher surfaces. Scale bar: 10 mm.

deep groove laterally between the epipophyses and postzygapophyses, which is most evident between the sixth and eighth cervical vertebrae of *Anhanguera* (Figures 7 and 8). Transverse-oblique crests in the mid-cervical vertebrae of *Anhanguera* and *Azhdarcho lancicollis* are similar to those present in *Caiman latirostris*, which are shorter and more concave than in extant birds (Figures 2, 3 and 7). The posterior cervical vertebrae of *Azhdarcho lancicollis* do not have preserved the regions of the transverse-oblique crests, but in both analyzed specimens of *Anhanguera* the crests are reduced in the eighth vertebra and absent in the ninth (Figure 8).

Craniolaterally in the axis of all analyzed pterosaurs, there is a tubercle (tax) and capitulum (cax) similar to those of extant archosaurs, which are more developed in *Anhanguera* sp. (AMNH 22555) and *Azhdarcho lancicollis* (Figures

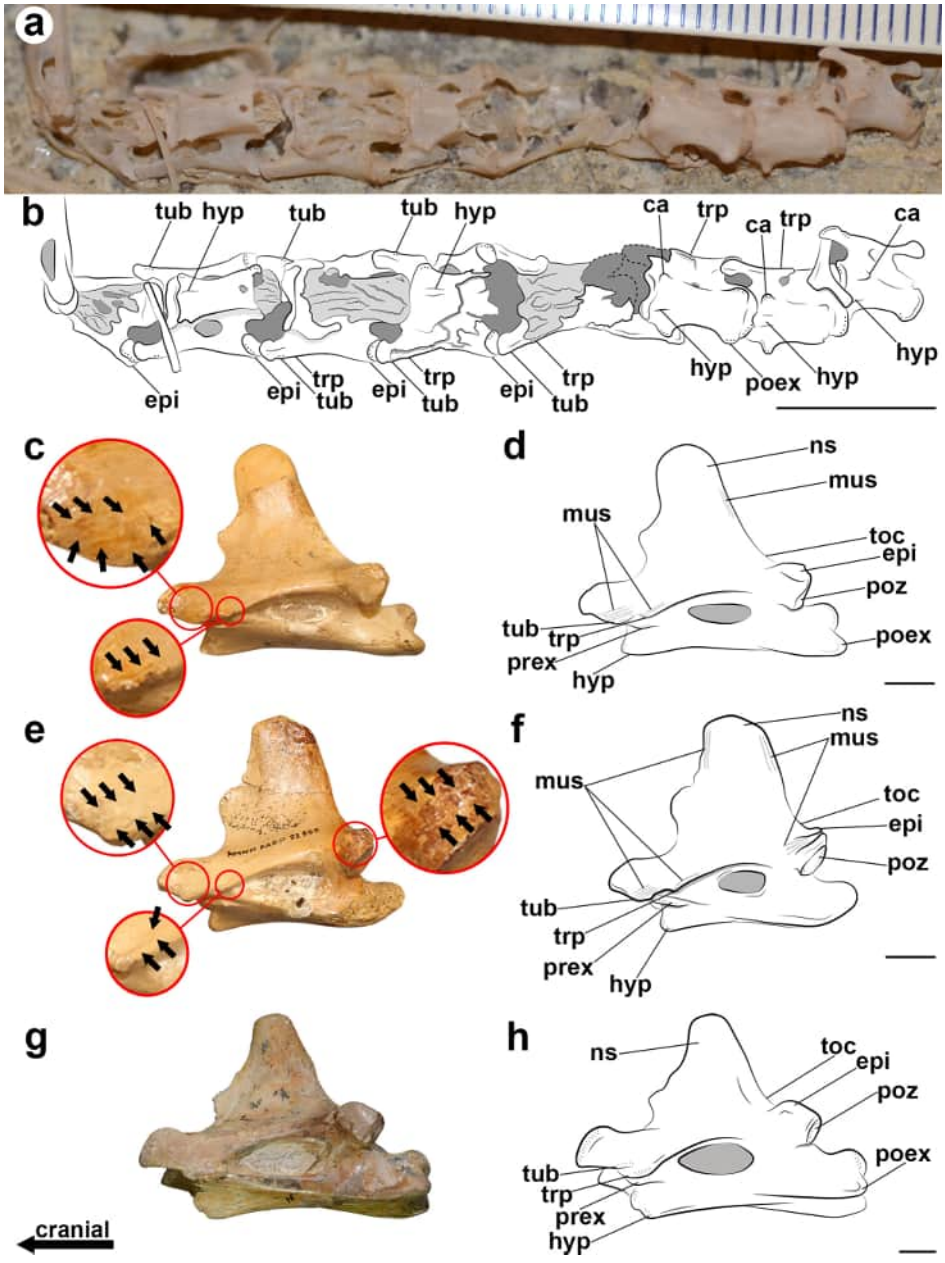

Figure 7. Photographs and interpretative drawings of the articulated cervical series of *Rhamphorhynchus muensteri*, which are presented from the atlas-axis to the sixth vertebra in ventral view and from the seventh to the ninth in left ventrolateral view (a, b); the fifth vertebra (c, d) and the sixth vertebra (e, f) of *Anhanguera* sp. (AMNH 22555) and the fourth vertebra of *Anhanguera piscator* (g, h) are in left lateral view. Arrows indicate muscle scars. Dotted regions indicate rougher surfaces. Broken regions in *Rhamphorhynchus muensteri* were represented in light gray and the plate is represented by dark gray (b). Scale bar: 10 mm.

1 and 6). In *Anhanguera* sp., the tubercle of the axis presents light muscular scars that extend dorsolaterally (Figure 6). We observed the presence of a *capitulum* in the entire cervical series of *Rhamphorhynchus muensteri*, which represents the articulation surfaces for the cervical ribs (Figure 7). In the region where we found the capitulum in *Rhamphorhynchus*, there are preexapophyses in the pterodactyloids analyzed.

Short, lateral bony structures that extend ventrolaterally in all postaxial vertebrae of the pterosaurs analyzed are defined here as tubercles, similar to the ones observed in *Caiman latirostris* and extant birds (Figures 7 and 8). The tubercles in *Rhamphorhynchus muensteri* (MGUH 1891.738), *Anhanguera* sp. (AMNH 22555), and *Anhanguera piscator* (NSM-PV 19892) have a rough surface (Figures 7 and 8). Uniquely in AMNH 22555, there are muscular scars extending

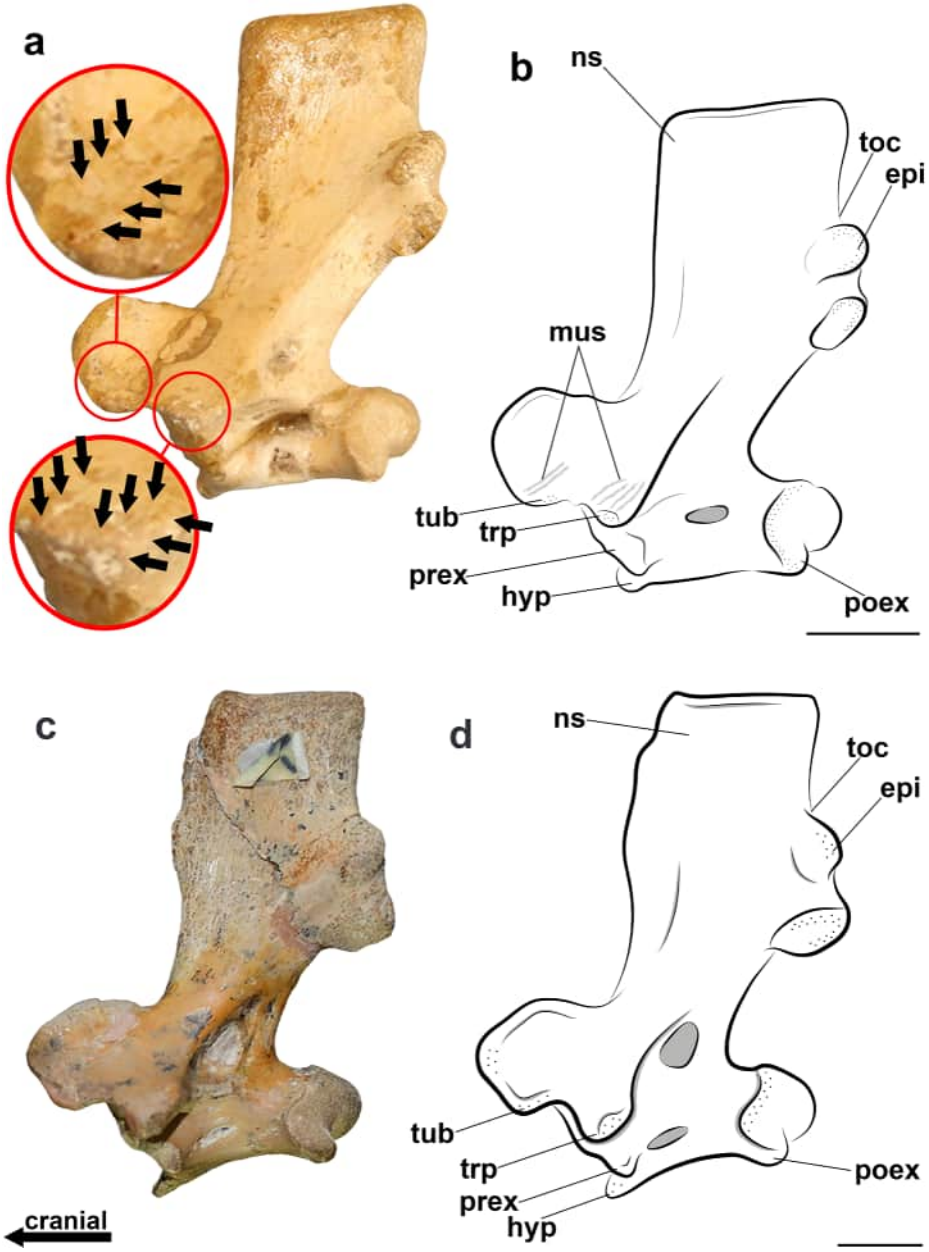

Figure 8. Photographs and interpretative drawings of the eighth cervical vertebra of *Anhanguera* sp. (AMNH 22555) (a, b) and *Anhanguera piscator* (c, d) in left lateral view. Arrows indicate muscle scars. Dotted regions indicate rougher surfaces. Scale bar: 10 mm.

ventrolaterally to the tubercles, as in the axis of this specimen (Figures 7 and 8). There are discrete transverse processes arranged caudally to the tubercles on the mid-cervical vertebrae, which are more developed in AMNH 22555 and NSM-PV 19892 (Figure 7). Subtle muscular scars are present dorsolaterally to the transverse processes of the mid-cervical vertebrae of AMNH 22555 (Figure 7). *Anhanguera* and *Azhdarcho lancicollis* have transverse processes longer than the tubercles in the posterior cervical vertebrae, as in the more posterior cervicals of extant birds (Figure 8). The transverse processes of all cervical vertebrae are rough at their ends (Figures 7 and 8).

The centrum of the atlas of *Anhanguera* and *Azhdarcho lancicollis* presents the cotyle expanded in the medial portion, thinning ventrally, and forming a process located on the cranioventral surface similar to a short hypapophysis (Figure 6). The atlas of these pterosaurs has lateral tubercles and a protruding dorsal surface, which resembles the muscle attachment sites in the vertebrae of *Caiman latirostris* and birds (Figures 1 and 6). In the postaxial cervical vertebrae, the hypapophyses are well-developed ventrocranially, as in extant archosaurs, and are longer in the mid-cervicals (Figure 7). The hypapophysis of the pterosaur eighth vertebra is pronounced and extends cranioventrally, and it is wider than the hypapophyses present in the mid-cervicals (Figure 8). In all analyzed pterosaurs, the preexapophyses are located laterally to the hypapophysis of each vertebra, as the capitulum of extant archosaurs (Figures 2, 3, 7 and 8). In the analyzed pterodactyloids, the preexapophyses of the eighth vertebra are longer than those of the ninth, but the hypapophyses and preexapophyses of the posterior cervicals are not as developed as in the mid-cervicals (Figure 7 and 8).

Cervical musculature reconstruction

Epaxial muscles

Transversospinalis group

Transversospinalis capitis

Rough areas and grooves on the top of the neural spines were the probable origins of these muscles (Figure 9). These attachments were fixed by aponeuroses from the axis to the first dorsal (or notarial) vertebra (Figure 10a), as observed in extant crocodylians. These osteological correlates are found even among the mid-cervical vertebrae of *Azhdarcho lancicollis*, which have extremely reduced neural spines. The broad areas of origin in the neural spines of the first dorsal (or notarial) vertebra and posterior cervical vertebrae indicate that the muscle was more robust in this region. The insertion was probably fleshy and was attached laterally to the dorsal surface of the supraoccipital crest of the skull, which has well-demarcated muscular scars in *Anhanguera piscator* (Figure 11). The suggested insertion site agrees with that observed in extant birds and crocodylians. We suggest that the muscular arrangement originated from nine muscular branches that come together in a belly to insert as a single bundle. We consider the presence of the muscle as a level I inference by the EPB (Table I), being homologous to the *transversospinalis capitis* of extant crocodylians and the *biventer cervicis* of extant birds, although the latter originates from osteological attachments only in the first thoracic (or notarial) vertebra.

Complexus

The developed and rough tubercles and epipophyses in the pterosaur mid-cervical vertebrae are consistent with the places of origin of this muscle in extant archosaurs (Figure 9).

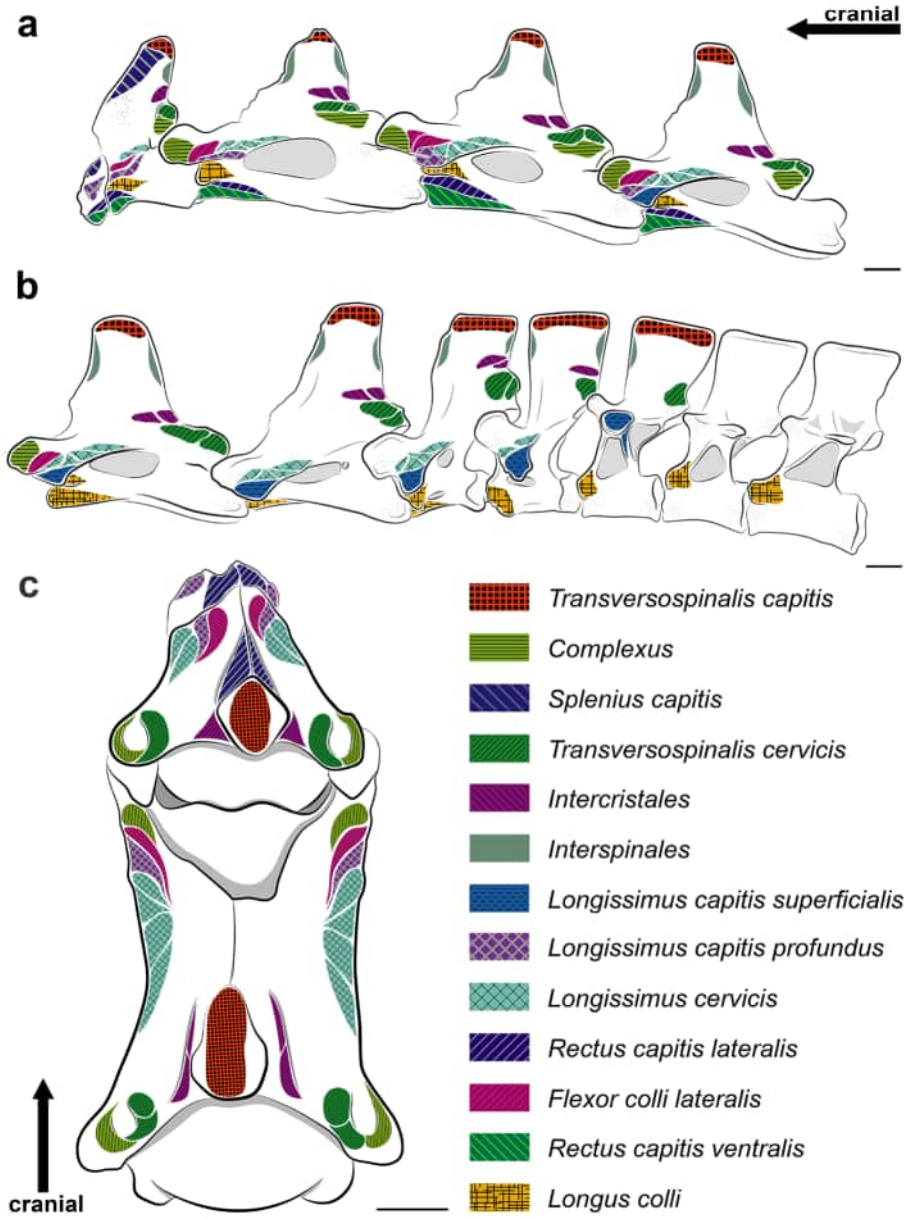

Figure 9. Locations of muscular attachments in the cervical vertebral column of *Anhanguera piscator*. Interpretative drawings of the cervical series from atlas to fifth vertebra (a) and cervical series from sixth to first dorsal vertebrae (b) in lateral view; interpretative drawings of the atlas, axis, and third vertebra in dorsal view (c). Scale bar: 10 mm.

The origins were probably fixed on the lateral edge of the tubercles from the third to the sixth vertebra and at the bases of the epipophyses from the axis to the fifth vertebra, which means that the muscle only extended along the cranial half of the neck (Figure 10a). The similarity of the correlates observed in pterosaurs with those presented by extant birds indicates that the origins were fixed by aponeuroses, although in extant crocodylians the origins are tendinous. Muscle scars that border both surfaces of the *crista nuchalis transversa* in the occipital region of the skull of *Anhanguera piscator* are consistent with the insertion area of this muscle (Figure 11). We suggest that the muscular arrangement originated from eight branches that joined together and formed a robust belly with a probably fleshy insertion. According to the similarities with the osteological correlates, the muscle was probably homologous to the *complexus* and *transversospinalis capitis* of extant birds and crocodylians, respectively,

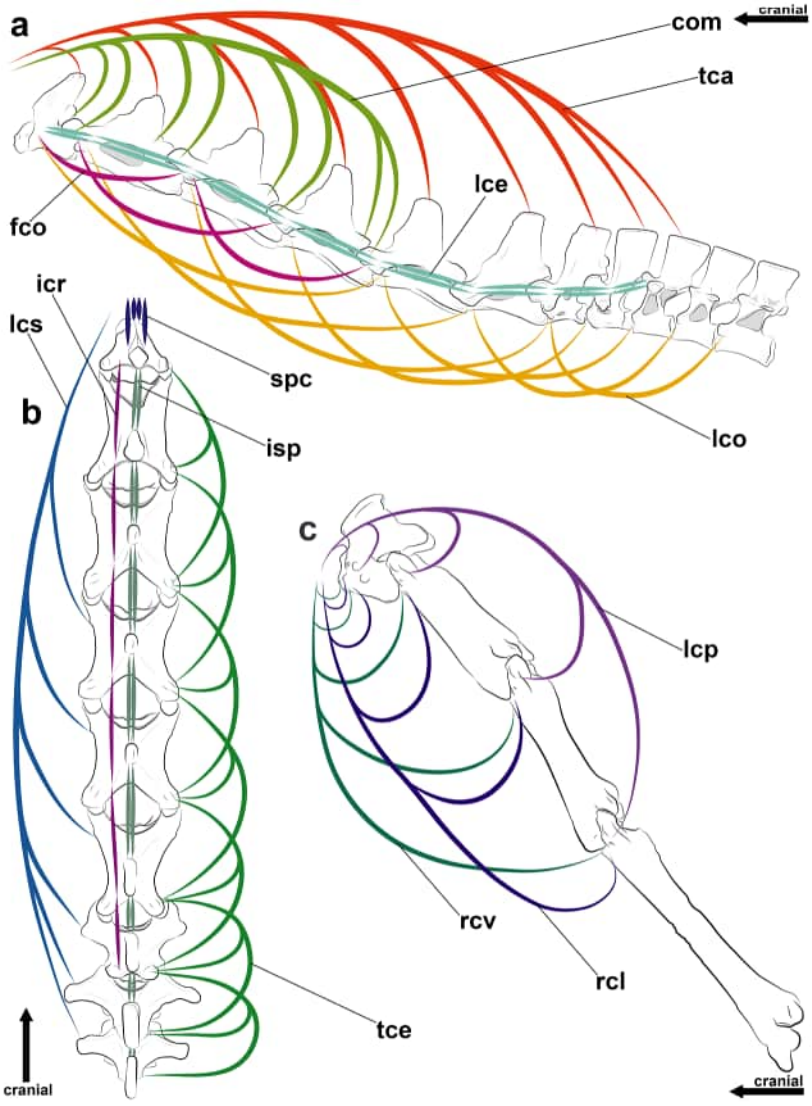

Figure 10. Extent of the inferred cervical muscles. Interpretive drawings of the cervical series of *Anhanguera piscator* in left lateral (a) and dorsal (b) view. Cervical series from the atlas to the fifth cervical vertebra of *Azhdarcho lancicollis* in left lateral view (c). The muscles are shown unilaterally, except for the *splenius capitis* and *interspinales*.

representing a level I inference by the EPB (Table I).

Splenius capitis

The muscular scar present on the cranial surface of the neural arch of the axis and the prominent dorsal surface of the atlas probably corresponded to the places of origin of this muscle (Figures 6 and 9). Both origins were probably attached by aponeuroses, as in extant archosaurs. The wide depression in the supraoccipital in the skull of *Anhanguera piscator* indicates that the insertions of the *splenius capitis* probably bordered the *crista nuchalis transversa* and the supraoccipital crest up to the most dorsal portion of the paraoccipitals, in the opisthotic (Figure 11). We suggest that the muscular arrangement originated through two attachments and formed two robust bundles that overlapped each other and had a fleshy insertion. According to the osteological correlates identified, this muscle was probably homologous to the *splenius capitis* of extant birds and to the *epistropheo-capitis* and *atloïdo-capitis* of extant crocodylians, which we consider a level I inference by the EPB (Table I). With attachment locations similar to

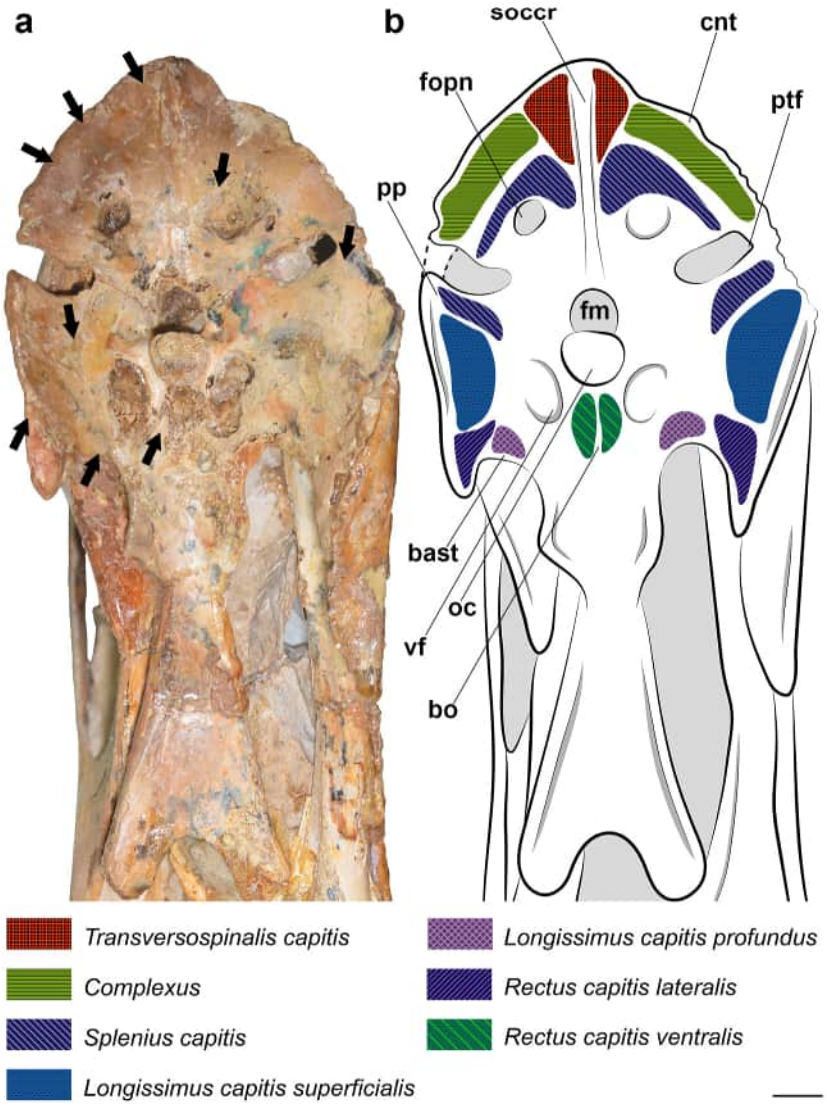

Figure 11. Photography (a) and interpretative drawing with locations of muscular insertions (b) of the occipital region of the skull of *Anhanguera piscator*. Arrows indicate muscle scars. Scale bar: 10 mm.

the *splenius capitis* of birds, we assume that this muscle had fibers oriented at 60° to its long axis in pterosaurs.

Transversospinalis cervicis

The presence of rough areas on the sides of the extremely developed epipophyses in all cervical vertebrae of *Anhanguera* and *Azhdarcho lancicollis* supports them as the sites of origins and insertions of this muscle, as in extant archosaurs (Figure 9). The tall, robust neural spines of *Anhanguera* sp. and *Anhanguera piscator* probably contributed an additional area for muscular attachment, as in extant crocodylians and in vertebrae of the first and third neck segments of extant birds. A prominence of the neural spine at the caudal end of the mid-cervical vertebrae of *Azhdarcho lancicollis* may also have been an additional area of attachment for the muscle and may have prevented its reduction in size. The muscular origins were probably connected by aponeuroses from the first dorsal (or notarial) vertebra to the third cervical vertebra, while the insertions were tendinous and attached from the eighth cervical vertebra to the axis (Figure 10b). The preservation

Table I. Level of inference according to the EPB, locations of cervical muscle attachments, and function of the muscles of the analyzed extant archosaurs and pterosaurs.

Muscle attachment	Attachment site in crocodylians	Attachment site in birds	Attachment site in pterosaurs	EPB
Transversospinalis capitis				
Origin	Neural spine	Neural spine	Neural spine	I
Insertion	Supraoccipital crest	*Supraoccipital crest*	*Supraoccipital crest*	I
Function	Dorsal flexion and yaw of the head.			
Complexus				
Origin	Epipophyses and lateral crest	*Torus dorsalis* and lateral crest	Epipophyses and lateral crest	I
Insertion	Crista nuchalis transversa	*Crista nuchalis transversa*	*Crista nuchalis transversa*	I
Function	Dorsal flexion, yaw, and roll of the head.			
Splenius capitis				
Origin	Neural spine	Neural spine	Neural spine	I
Insertion	Paraoccipital process	Supraoccipital and paraoccipital process	Supraoccipital and paraoccipital process	I
Function	Dorsal flexion and lateral stability of the head.			
Transversopinalis cervicis				
Origin	Neural spine and epipophyses	Neural spine and *torus dorsalis*	Neural spine and epipophyses	I
Insertion	Neural spine and epipophyses	Neural spine and *torus dorsalis*	Neural spine and epipophyses	I
Function	Dorsal flexion and yaw of the cranial half of the neck.			
Intercristales				
Origin	Transverse oblique crest	Transverse oblique crest	Transverse oblique crest	I
Insertion	Transverse oblique crest	Transverse oblique crest	Transverse oblique crest	I
Function	Intervertebral dorsal flexion and cervical stabilization.			
Interspinales				
Origin	Neural spine	Neural spine	Neural spine	I
Insertion	Neural spine	Neural spine	Neural spine	I
Function	Intervertebral dorsal flexion and cervical stabilization.			
Longissimus capitis superficialis				
Origin	Transverse processes	Absent	Transverse processes	II
Insertion	Paraoccipital	Absent	Paraoccipital	II
Function	Yaw and roll of the head.			
Longissimus capitis profundus				

Table I. Continuation.

Origin	Transverse processes and tubercles	*Tuberculum ansae*	Transverse processes and tubercles	I
Insertion	Basal tubera	Basal tubera	Basal tubera	I
Function	Ventral flexion and roll of the head.			
Longissimus cervicis				
Origin	Transverse process and lateral of neural arch	Transverse process, lateral crest and costal process	Transverse processes and lateral of neural arch	I
Insertion	Transverse process, lateral crest and cervical ribs	Transverse process, lateral crest and costal process	Transverse processes and lateral of neural arch	I
Function	Ventral flexion, yaw, and stability of the neck.			
Flexor colli				
Origin	Tubercles	*Tuberculum ansae*	Tubercles	I
Insertion	Transverse processes and tubercles	Costal process	Transverse processes and tubercles	I
Function	Ventral flexion of the cranial half of the neck.			
Rectus capitis lateralis				
Origin	Hypapophysis and capitular process	Hypapophysis	Hypapophysis and preexapophyses	I
Insertion	Paraoccipital	Paraoccipital	Paraoccipital	I
Function	Yaw and roll of the head.			
Rectus capitis ventralis				
Origin	Hypapophysis	Hypapophysis	Hypapophysis	I
Insertion	Basioccipital	Basioccipital	Basioccipital	I
Function	Ventral flexion of the head			
Longus colli				
Origin	Hypapophysis and capitular process	Hypapophysis	Hypapophysis and preexapophyses	I
Insertion	Cervical ribs	Lateral crest and costal process	Preexapophyses and/or cervical ribs	I
Function	Ventral flexion of the neck			

of MGUH 1891.738 makes it difficult to visualize the correlates in the mid-cervical vertebrae (Figure 7a and 7b). However, we observed developed epipophyses in the seventh, eighth, and ninth vertebrae, which support the presence of the most caudal origins and insertions of this muscle in *Rhamphorhynchus* (Figure 7a and 7b). Furthermore, all vertebrae of MGUH 1891.738 had tall neural spines, which also matches the area of this muscle's attachment. The suggested muscular arrangement shows that the origins were composed of fourteen bundles that attached to adjacent vertebrae, with each pair of bundles resulting in a single insertion into the subsequent vertebrae. Correlates support that the pterosaur *transversospinalis cervicis* was likely homologous to the *longus colli dorsalis*, *pars cranialis*, *caudalis*, and *profunda* of extant

birds, and *transversospinalis cervicis* of extant crocodylians, which indicates a level I inference by the EPB (Table I).

Intercristales

The origins and insertions of this muscle were probably fixed by aponeuroses on the prominent transverse oblique crests that are present caudolaterally to the bases of the neural spines of the cervical vertebrae of *Anhanguera* and *Azhdarcho lancicollis* (Figure 9). The origins of this muscle were present from the third to the eighth cervical vertebra, while the insertions were arranged from the axis to the seventh cervical vertebra (Figure 10b). Poor preservation of the mid-cervical vertebrae of MGUH 1891.738 made it difficult to identify the osteological correlates corresponding to the attachment sites of this muscle (Figure 7a and 7b). However, developed transverse oblique crests on the posterior cervical vertebrae of this specimen indicate that the muscle was also present in *Rhamphorhynchus muensteri* (Figure 7a and 7b). We suggest that the muscular arrangement was formed by six bundles that originated and were inserted on adjacent vertebrae. They were likely homologous to the *intercristales* and *interarticulares* of extant birds and crocodylians, respectively, representing a level I inference by the EPB (Table I).

Interspinales

The muscles probably had fleshy attachments in the lateral grooves on the cranial and caudal surfaces of the neural spines of the cervical vertebrae, as seen throughout the entire cervical series of extant crocodylians and in the first cervical segment of extant birds (Figures 2, 3 and 9). These correlates are also seen in the cranial and caudal ends of the reduced neural spines of the mid-cervical vertebrae of *Azhdarcho lancicollis*, which is consistent with the presence of these muscles. The muscular segments originated from the third cervical vertebra to the first dorsal (or notarial) vertebra, while the insertions were fixed from the axis to the ninth cervical vertebra (Figure 10b). We suggest that the muscular arrangement was composed of eight thin bundles that connected to adjacent vertebrae. These muscles are homologous to the *interspinales* of extant birds and crocodylians, which supports their presence as a level I inference by the EPB (Table I).

Longissimus and *Iliocostalis* groups

Longissimus capitis superficialis

The muscle originated in grooves present on the lateroventral surface of the developed transverse processes of the vertebrae, as is also seen in extant crocodylians. (Figures 2 and 9). The origins were fixed by aponeuroses, probably from the fifth cervical to the first dorsal (or notarial) vertebrae (Figure 10b). The presence of the muscle is corroborated in MGUH 1891.738 by the developed transverse processes from the fifth vertebra onwards, although the preservation of the material in a slab makes analysis difficult (Figure 7a and 7b). The broad edges of the opisthotics in the skull of *Anhanguera piscator* formed extensive paraoccipital processes, which probably provided a broad area for aponeurotic attachments of this muscle (Figure 11). We suggest that the muscular arrangement was composed of six branches that joined into a robust belly and inserted on the skull as a single bundle. Apparently, there is no homologue of this muscle in extant birds, which is consistent with a level II inference by the EPB in this case (Table I).

Longissimus capitis profundus

This muscle probably originated on the lateral edges of the short transverse processes and

tubercles in the cranial half of the pterosaur neck, as also seen in the vertebrae of extant archosaurs (Figure 9). In extant birds, the origins also occur on the costal processes, which, among the pterosaurs analyzed, are present as cervical ribs only in *Rhamphorhynchus muensteri* (Figure 7a and 7b). The origins in pterosaurs were likely fixed by aponeuroses from the atlas to the fifth vertebra (Figure 10c). Probably, the *basal tubera* developed on the basioccipitals in *Anhanguera piscator* were the sites of the tendinous insertion of this muscle, as in extant birds and crocodylians (Figure 11). We suggest that the muscular arrangement was composed of five short bundles that formed a thin belly that inserted through a single narrow tendon. The restriction of the origins of the *longissimus capitis profundus* to only the first half of the neck is also observed in both extant archosaurs. The muscle is homologous to the *rectus capitis dorsalis* and *longissimus capitis profundus* of extant birds and crocodylians, respectively, representing a level I inference by the EPB (Table I).

Longissimus cervicis

The muscle had tendinous origins, which were probably attached to the laterocranial surface of the base of the transverse processes and cranially to the lateral crest (Figure 9). The origins were fixed from the third cervical to the first dorsal (or notarial) vertebra (Figure 10a). The insertions were aponeurotic and fixed laterocaudally on the transverse processes and on the caudal portion of the lateral crest (Figure 9), from the axis to the ninth cervical vertebra (Figure 10a). We suggest that the arrangement corresponded to muscular segments composed of two thin bundles that originated and inserted on adjacent vertebrae (Figure 10a). The arrangement formed by two muscle bundles differs from what is observed in extant archosaurs, in which these muscles are composed of more bundles. This means that the muscle in pterosaurs was thinner than in extant archosaurs, especially considering the small size and proximity between attachment sites. This muscle is homologous to the *longissimus cervicis* of extant crocodylians and to portions of the *intertransversarii* observed in extant birds, which represents a level I inference by the EPB (Table I). Due to the similarity in attachment locations with the *longissimus cervicis* of *Caiman latirostris*, we assume that this muscle in pterosaurs had fibers parallel to its long axis.

Flexor colli

This muscle was possibly attached by aponeuroses to all vertebrae that had laterally developed tubercles (Figure 9). These attachments probably bordered the ones of the *longissimus capitis profundus*, as in extant birds and crocodylians (Figure 9). We consider that the origins were fixed from the fourth to the sixth, while the insertions were fixed from the axis to the fourth vertebra (Figure 10a). The arrangement suggests that the muscle originated and inserted by three bundles, which were joined by a thin muscular belly. The muscle is homologous to the portion of the *longissimus cervicis* and *flexor colli lateralis* of extant crocodylians and birds, respectively, representing a level I inference by the EPB (Table I).

Hypaxial muscles

Rectus capitis lateralis

The muscle probably originated from aponeuroses on the sides of the hypapophyses and ventral surfaces of the preexapophyses (Figure 9a and 9b). The more prominent hypapophyses of the mid-cervical vertebrae were possibly related to the more caudal origins of this muscle (Figure 9a and 9b). In *Rhamphorhynchus muensteri*, the origins of this muscle may have had additional

attachments to the ventral surfaces of the *capitulum* (Figure 7a and 7b). The origins were possibly established from the atlas to the fifth cervical vertebra in the analyzed pterosaurs (Figure 10c). The muscle probably had fleshy insertions on the pronounced ventral margins of the paraoccipital processes, as those seen in the skull of *Anhanguera piscator* (Figure 11). We suggest that the muscular arrangement was composed of five short bundles that formed a slender belly with a single, narrow insertion. It is probably homologous to the *rectus capitis lateralis* and to a portion of the *iliocostalis capitis* in extant birds and crocodylians, respectively. Therefore, we assume the presence of the muscle as a level I inference by the EPB (Table I).

Rectus capitis ventralis

The muscle probably had aponeurotic origins that were attached to the medial surface of the hypapophyses (Figure 9a and 9b). Like the *rectus capitis lateralis*, we suggest that the most caudal origins were attached to cervical vertebrae that had more developed hypapophyses (Figure 9a and 9b). The origins were attached from the atlas to the fifth vertebra (Figure 10c). It probably inserted via a tendon that attached to the depression on the mid-ventral surface of the basioccipital, as seen in the skull of *Anhanguera piscator* (Figure 11). We suggest that the muscular arrangement was composed of five bundles that formed a belly with a single insertion. It is homologous to the *rectus capitis ventralis*, which attaches to the hypapophyses of the vertebrae of extant birds, and to the *rectus capitis anticus major*, which attaches to the ventral processes of the vertebrae of extant crocodylians. In both extant taxa, the insertion is concentrated on the mid-ventral portion of the basioccipital, as we suggest in *Anhanguera piscator*. Therefore, the muscle insertions described here can be considered an EPB inference level I (Table I).

Longus colli

The muscle probably originated on the prominent hypapophyses of the vertebrae of the caudal half of the neck and on the developed capitular processes of the posterior cervical and of the most cranial dorsal vertebrae (Figure 9a and 9b). The origins were fleshy and attached from the sixth cervical to the third dorsal (or notarial) vertebra (Figure 10a). The well-developed preexapophyses of the cervical vertebrae were probably insertion sites for this muscle (Figure 9a and 9b). The bases of the cervical ribs of *Rhamphorhynchus muensteri* were probably additional attachment sites, as in extant crocodylians (Figures 1, 2, 7a and 7b). The insertions were established by aponeuroses from the axis to the fifth cervical vertebra (Figure 10a). We suggest that the muscular arrangement originated from seven bundles that formed a belly and branched cranially into four insertion bundles. It is probably homologous to *longus colli ventralis* and to the portions of the *longus colli* in extant birds and crocodylians, respectively, which represents a level I inference by the EPB (Table I).

Volume and Maximum Force Production (F_{pmax}) of the muscles

To delimit the outer edge of the musculature in the pterosaur cervical reconstruction, we positioned polygonal hoops around the vertebrae following the standard dimension seen in extant archosaurs, in which the total width and height of the neck represents a 50% increase in relation to the vertebral width (Figure 12, Table SII).

The limits of contact between the muscles themselves were established according to the maximum thickness presented by each one

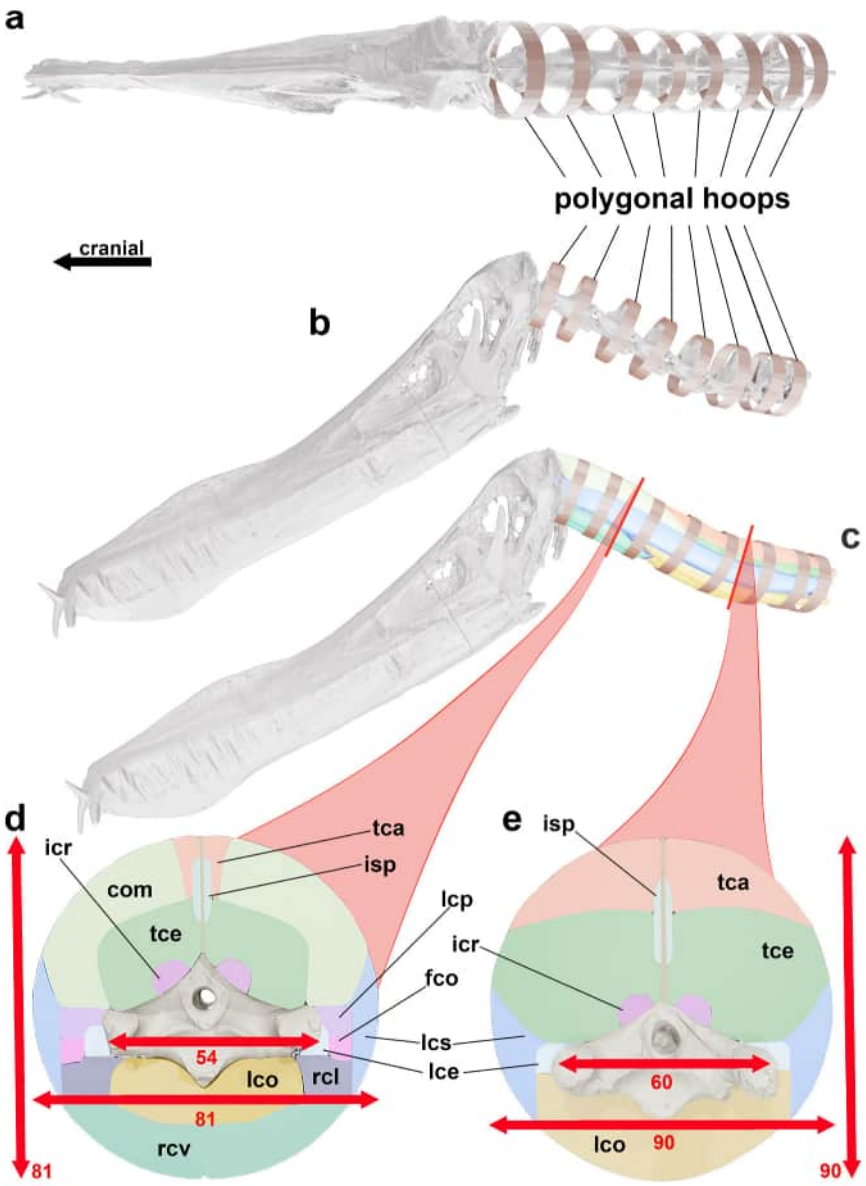

Figure 12. Three-dimensional reconstructions of the neck of *Anhanguera piscator*. Polygonal hoops used to demarcate the muscular limits and arrangement of the muscles in dorsal (a) and left lateral (b) views. Arrangement of the cervical muscles in left lateral view (c). Cross-sections of the neck showing the proportion between the space occupied by muscles and bone in the regions of the fourth (d) and seventh (e) cervical vertebrae in cranial view. Red bar (c) indicates the location of the cross section shown. Red arrows (d, e) indicate the dimensions. Measurements (d, e) are shown in millimeters.

(Figure 12, Table SIII). Considering the pattern observed in the thickness of the muscle bundles of extant birds, in pterosaurs the areas of muscular origin represent the maximum thickness of the bundles (Table SIII). Therefore, the sum of the thickness of the muscular bundles in the regions where they were concentrated determines the maximum thickness of each cervical muscle of pterosaurs (Figure 12, Table SIII). The *complexus*, *longissimus capitis profundus*, *flexor colli*, *rectus capitis lateralis*, and *rectus capitis ventralis* had the muscle bundle arrangement concentrated close to the third and fourth cervical vertebrae of pterosaurs (Figure 12). The developed osteological correlates and the number of clustered muscle bundles indicate that the *complexus* was the thickest muscle in the cranial half of the neck (Figure 12, Table SIII). The wide area of the attachment sites and the concentration of bundles also indicate that the *rectus capitis ventralis* was robust, being the thickest among the hypaxial muscles in the cranial half of the neck of pterosaurs (Figure 12, Table SIII).

Longer muscles concentrated their bundles near the sixth, seventh, and eighth cervical vertebrae of pterosaurs, such as the *transversospinalis capitis*, *transversospinalis cervicis*, *longissimus capitis superficialis*, and *longus colli* (Figure 12). The extensive overlapping of bundles and the broad areas of attachment of the origins of the *transversospinalis cervicis* and *longus colli* indicate that both were the thickest muscles of the neck, which is consistent with the broad dorsolateral and ventral regions of the mid-cervical vertebrae that accommodated their muscular bellies (Figure 12, Table SIII). The well-marked correlates in the transverse processes and the overlapping of the muscle bundles in all the extent of the neck suggest that the *longissimus capitis superficialis* was the most robust muscle arranged laterally to the cervical series (Figure 12, Table SIII). The segmented muscles were composed of one or two bundles per segment, which indicates that they tend to be thinner than the other muscles. However, these muscles probably reached their maximum thickness between the sixth and eighth cervical vertebrae, as indicated by the larger attachment areas in the osteological correlates (Figure 12, Table SIII). The wide insertion areas of the *splenius capitis* demonstrate that this may have been its thickest portion, since these areas indicate that the muscle also had triangular bundles, as in extant archosaurs (Figure 11). After establishing the bundles' muscular path, the limits inferred by the maximum thickness of each muscle, together with the limit imposed by the vertebrae's cortex and externally by the polygonal hoops, allowed us to define the

Table II. Estimated volume, total fiber length, and maximum force (F_{pmax}) for each inferred cervical muscle.

	volume (cm^3)	total fiber length (cm)	F_{pmax} (N)
Anhanguera piscator			
Transversospinalis capitis	33.3249	40.562	23.252
Complexus	75.7021	22.618	94.726
Transversospinalis cervicis	82.8938	37.162	63.130
Splenius capitis	16.988	2.562	93.831
Intercristales	15.6777	31.819	13.945
Interspinales	1.5621	22.135	1.997
Longissimus capitis superficialis	60.173	39.118	43.535
Longissimus capitis profundus	10.3764	15.498	18.949
Longissimus cervicis	26.6115	37.004	20.353
Flexor colli	10.3548	19.753	14.836
Rectus capitis lateralis	9.8984	15.320	18.243
Rectus capitis ventralis	50.1921	15.452	91.932
Longus colli	107.7309	40.449	75.378

Table II. Continuation.

Azhdarcho lancicollis			
Transversospinalis capitis	30.5379	41.485	20.833
Complexus	12.1323	15.337	22.388
Transversospinalis cervicis	49.4169	36.722	38.085
Splenius capitis	2.3907	2.028	16.681
Intercristales	0.6870	34.862	0.557
Interspinales	0.1129	10.053	0.317
Longissimus capitis superficialis	26.0825	38.237	19.305
Longissimus capitis profundus	3.0645	14.032	6.181
Longissimus cervicis	10.7957	37.374	8.175
Flexor colli	3.8783	21.590	5.084
Rectus capitis lateralis	6.2691	13.322	13.318
Rectus capitis ventralis	11.9221	13.617	24.779
Longus colli	60.4741	39.926	42.867
Rhamphorhynchus muensteri			
Transversospinalis capitis	2.1398	12.263	4.938
Complexus	1.3339	6.574	5.742
Transversospinalis cervicis	1.9079	11.688	4.620
Splenius capitis	0.2423	0.759	4.517
Intercristales	0.0347	8.908	0.110
Interspinales	0.0092	7.011	0.037
Longissimus capitis superficialis	1.0809	11.517	2.656
Longissimus capitis profundus	0.3868	4.526	2.419
Longissimus cervicis	0.7797	10.924	2.020
Flexor colli	0.2735	5.490	1.410
Rectus capitis lateralis	0.2097	4.394	1.351
Rectus capitis ventralis	1.1423	4.422	7.661
Longus colli	2.4212	12.338	5.554

This table disregards the bilateral arrangement of muscles.

volume of each muscle (Figure 12), which were quantified and are shown in Table II.

According to our inferred cervical muscular arrangement, the area occupied by the epaxial muscles in any region of the neck was larger than that of the hypaxial muscles, being approximately double in *Anhanguera piscator* and *Rhamphorhynchus muensteri* (Figure 12), due to the large volume of the *transversospinalis* muscles (*transversospinalis capitis*, *complexus*, *splenius capitis*, and *transversospinalis cervicis*) and the number of epaxial muscles in relation to the hypaxials (Figure 12). According to F_{pmax}, the *complexus*, *transversospinalis cervicis*, *rectus capitis ventralis*, and *longus colli* muscles were often the most forceful, being mainly responsible for elevating the head and neck (Table II). Specifically, the *complexus* and *rectus capitis ventralis*, responsible for pitching of the head, had the greatest F_{pmax} in *Anhanguera piscator* and *Rhamphorhynchus muensteri*, while the *transversospinalis cervicis* and *longus colli*, responsible for pitching of the neck, had the greatest F_{pmax} in *Azhdarcho lancicollis*. The *transversospinalis capitis* was responsible for dorsiflexion of the head and was also a powerful muscle, especially in *Rhamphorhynchus muensteri*.

Among the more deeply arranged muscles, the *splenius capitis* was located dorsomedially to the cervical series and was limited to between the occipital region of the skull and the axis (Figure 13). Despite being short, the F_{pmax} indicates that the *splenius capitis* contracted with substantial force, especially in *Anhanguera piscator* (Table II), although this does not confirm that it could actually perform a positive work. The *interspinales*, *intercristales*, and *longissimus cervicis* muscles were probably segmented muscles, arranged deeply and throughout the entire length of the neck (Figure 13). These three muscles surrounded the surfaces of the vertebral neural arch: the *interspinales* occupied the region between the neural spines, the *intercristales* were arranged laterally to the base of the neural spines, and the *longissimus cervicis* were present laterally to the neural arch of the cervical series (Figure 13). The *interspinales* and *intercristales* were the muscles that had lowest force-generating potentials according to their F_{pmax} (Table II). Laterally, the *longissimus cervicis* was the main muscle responsible for cervical yaw and also presented a low F_{pmax}, which is possibly related to the segmented arrangement. The deeper muscle was the *longus colli*, which probably covered the ventral surface of the cervical vertebrae along the entire length of the neck (Figure 13). The *longus colli* was probably the most voluminous muscle of the neck in the analyzed pterosaurs and the most forceful of *Azhdarcho lancicollis* (Table II).

The *transversospinalis cervicis* wrapped around the dorsolateral surface of the neural arch and completely overlapped the *intercristales* and the most ventral portion of the *interspinales* (Figure 14). The *transversospinalis cervicis* were probably the most voluminous among the epaxial muscles of pterosaurs and had the greatest F_{pmax} of the epaxial muscles of *Azhdarcho lancicollis* (Table II).

The *longissimus capitis profundus*, *flexor colli*, *rectus capitis lateralis*, and *recuts capitis ventralis* were present from the most cranial region to the middle of the neck (Figure 14). The *longissimus capitis profundus* and *flexor colli* were positioned lateral to the cervical series, which indicates that both overlapped the *longissimus cervicis* in the cranial half of the neck (Figure 14). The *longissimus capitis profundus* and *flexor colli* had extremely low F_{pmax} compared to other muscles responsible for the ventral flexion of the skull and neck (Table II).

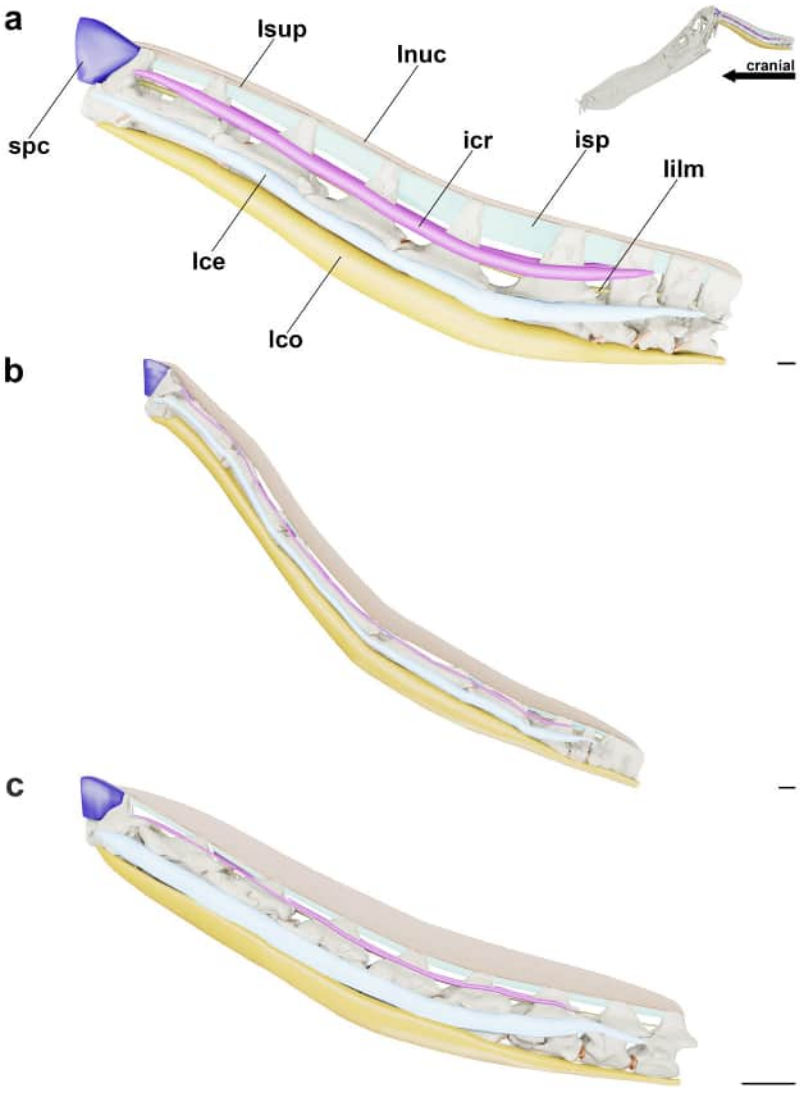

Figure 13. Reconstructions of the deep cervical musculature of *Anhanguera piscator* (a), *Azhdarcho lancicollis* (b), and *Rhamphorhyinchus muensteri* (c) in left lateral view. The *transversospinalis capitis*, *complexus*, *transversospinalis cervicis*, *longissimus capitis superficialis*, *longissimus capitis profundus*, *flexor colli*, *rectus capitis lateralis*, and *rectus capitis ventralis* are omitted. Scale bar: 10 mm.

In turn, the *rectus capitis lateralis* and *rectus capitis ventralis* were arranged ventrolaterally and ventral to the neck, respectively, overlapping the *longus colli* up to the middle of the neck (Figure 14). The *rectus capitis lateralis* probably had a considerably lower volume and F_{pmax} than the *rectus capitis ventralis*, although both were inferred to have a similar length (Table II). The *rectus capitis ventralis* was the most superficial muscle arranged ventrally and was among the most voluminous of the neck, being thicker than the bundles of the *longus colli* in the cranial half of the neck (Table II, Figure 14). In *Rhamphorhynchus muensteri*, the *rectus capitis ventralis* had the greatest F_{pmax} of all neck muscles, while in *Anhanguera piscator*, it produced the greatest force among the hypaxials.

The *transversospinalis capitis* were the most superficial of the dorsal muscles, being arranged along the entire cervical length (Figure 15). Their bundles overlapped the dorsal surfaces of the *splenius capitis*, dorsal and lateral surfaces of the *interspinales*, and dorsal and dorsolateral surfaces of the *transversospinalis cervicis* (Figure 15). The volume and, consequently, F_{pmax} of the *transversospinalis capitis* indicates a robust muscle in *Rhamphorhynchus muensteri* and *Azhdarcho lancicollis* and a more gracile one in

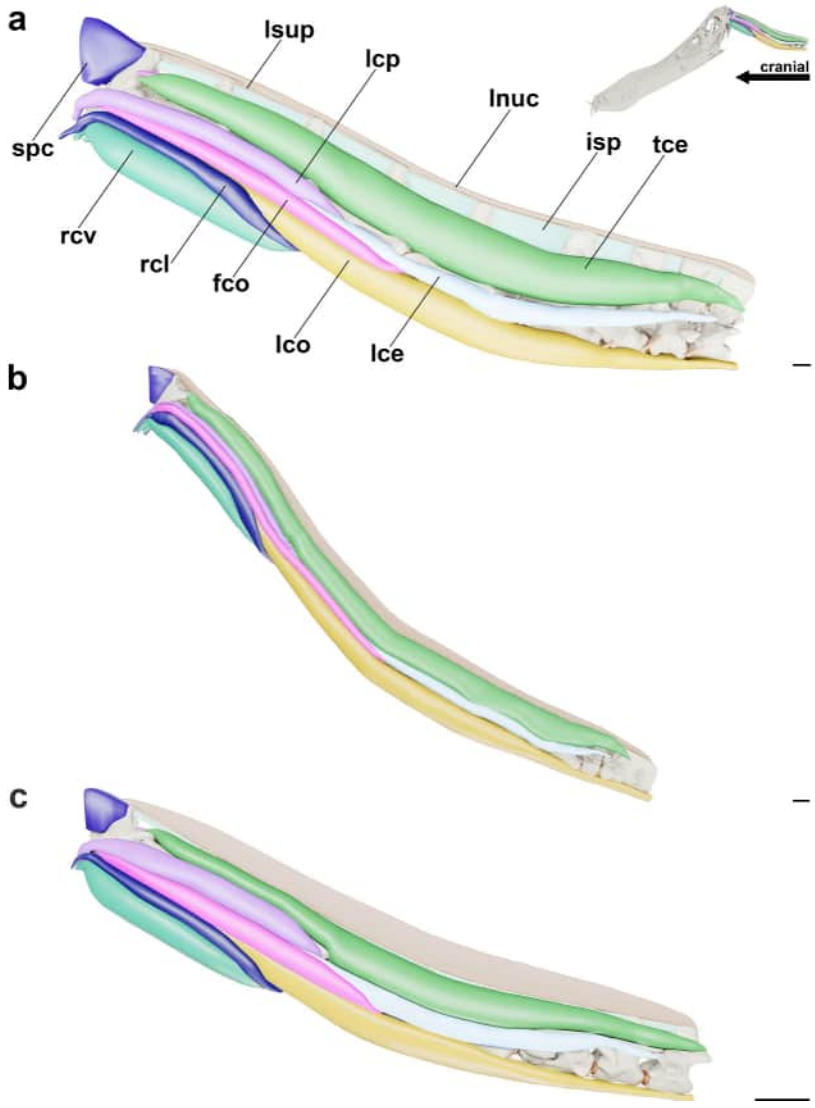

Figure 14. Reconstructions of the intermediate cervical musculature of *Anhanguera piscator* (a), *Azhdarcho lancicollis* (b), and *Rhamphorhyinchus muensteri* (c) in left lateral view. The *transversospinalis capitis*, *complexus*, and *longissimus capitis superficialis* are omitted. Scale bar: 10 mm.

Anhanguera, which is related to the differences in the anatomy of the neural spines of the cervical vertebrae of the different pterosaurs we analyzed (Table II).

The *complexus* were located superficially in the dorsolateral portion of the cranial half of the neck, overlapping the lateral surface of the *splenius capitis* and the *transversospinalis cervicis* in the cranial half of the neck (Figure 15). The *complexus* were among the most voluminous muscles, being the thickest cervical muscles in the cranial half of the neck (Table II). Furthermore, the *complexus* were the strongest neck muscle of *Anhanguera piscator* and the strongest among the epaxials of *Rhamphorhynchus muensteri* (Table II).

Finally, the *longissimus capitis superficialis* were probably the most superficial of the laterally-arranged muscles of the neck (Figure 15). They were arranged along the entire cervical length, overlapping the *longissimus capitis profundus*, *flexor colli*, *rectus capitis lateralis*, and the ventrolateral surface of the *transversospinalis cervicis* (Figure 15). The *longissimus capitis superficialis* was the strongest muscle among those arranged laterally to the cervical series (Table II).

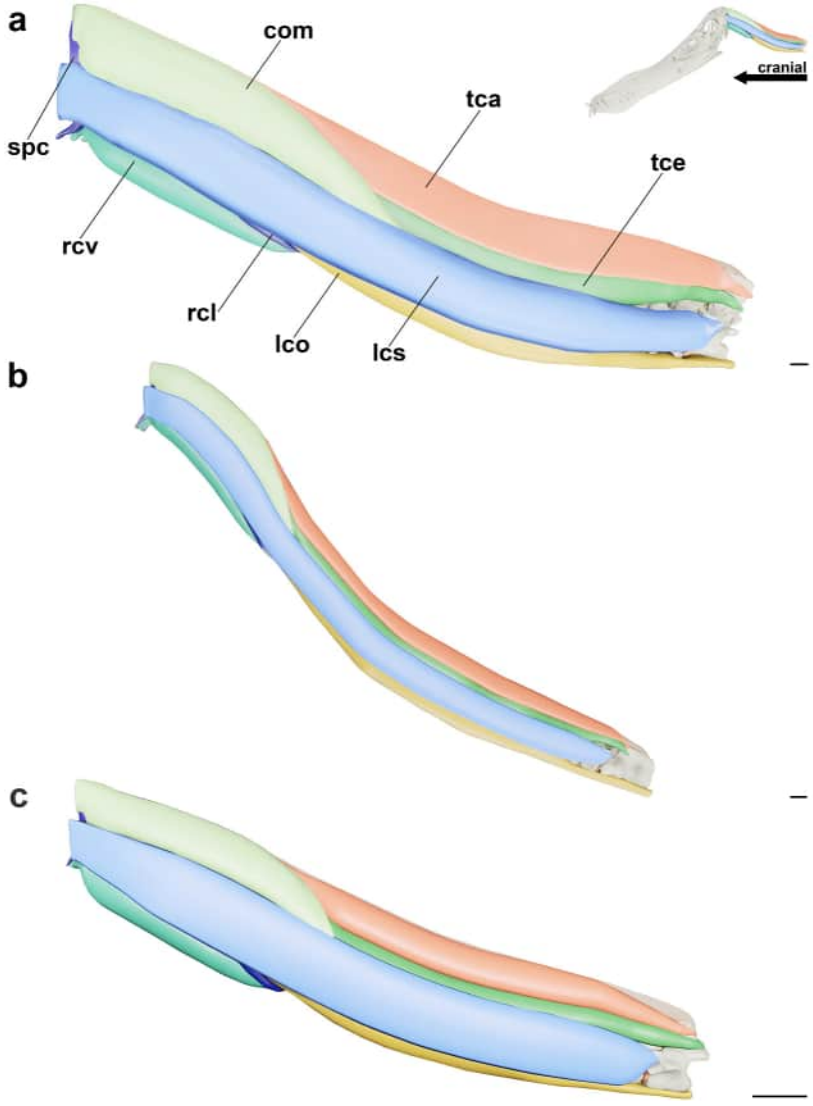

Figure 15. Reconstructions of the superficial cervical musculature of *Anhanguera piscator* (a), *Azhdarcho lancicollis* (b), and *Rhamphorhyinchus muensteri* (c) in left lateral view. Scale bar: 10 mm.

DISCUSSION

Of the thirteen pterosaur muscles we reconstructed here, only the *longissimus capitis superficialis* did not have an EPB level I inference because we could not recognize the correlate of the muscle attachment site in extant birds (Tsuihiji 2005, 2007, Snively & Russell 2007).

The *transversospinalis capitis*, *complexus*, *splenius capitis*, *longissimus capitis superficialis*, *longissimus capitis profundus*, *rectus capitis lateralis*, and *recuts capitis ventralis*, as we inferred here, make up the "craniocervical system" directly responsible for head movements (Zweers et al. 1987, Davies & Green 1994). The sturdiness and relatively high force potential we suggest for the muscles of the cranial half of the pterosaur neck are consistent with the broad insertion sites and scars present on the occipital region of *Anhanguera piscator* (Figure 5) (Witmer et al. 2003, Habib & Godfrey 2010). The extent of the supraoccipital crest, *crista nuchalis transversa*, and paraoccipital processes of *Anhanguera piscator* allowed wider insertion areas for the *transversospinalis capitis*, *complexus*, *longissimus capitis superficialis*, and *rectus capitis lateralis*, indicating that dorsal flexion, yaw, roll, and lateral head stability were

enhanced (Snively & Russell 2007, Snively et al. 2013, Böhmer et al. 2020).

Our inference of the *transversospinalis capitis* with a more medial insertion on the supraoccipital crest of *Anhanguera piscator* differs from the hypothesis of a dorsolateral insertion on the occipital region of the skull of the azhdarchid *Hatzegopteryx*, which would indicate an attachment on the edges of the nuchal crest (Naish & Witton 2017). Here, we assume that the *crista nuchalis transversa* anchored the insertion of the *complexus*, as in extant birds, because besides their role in dorsal flexion of the neck, the muscles attached to the broad crest would contribute greatly to the lateral movement of the skull (Burton 1974, Snively & Russell 2007). The wide depression that extends from the supraoccipital to the dorsal margin of the opisthotics indicates a wide insertion of the *splenius capitis*, which possibly accentuated dorsal and lateral flexion and provided more lateral stability to the head (Snively & Russell 2007, Böhmer et al. 2020).

The insertion of the *longissimus capitis superficialis* associated with muscle scars on the paraoccipital processes of *Anhanguera piscator* differs from the hypothesis that this osteological correlate would be the insertion site of the *spino-capitis posticus* (Naish & Witton 2017). In any case, either the *longissimus capitis superficialis* or the *spino-capitis posticus* would dorsally and/or laterally flex the skull, as observed along the cervical series in extant crocodylians (Cleuren & De Vree 2000, Tsuihiji 2005, 2007, Snively & Russell 2007). The F_{pmax} obtained for the *longissimus capitis superficialis* indicates a great yaw of the skull, which could be improved by the unilateral flexion capacity of the *complexus* (Table II). According to the insertion sites, the contraction of the *longissimus capitis superficialis* and *rectus capitis lateralis* could still promote skull roll, which, according to F_{pmax}, would be a more moderate movement than the lateral flexions (Table II). The insertion of the *longissimus capitis profundus* and *rectus capitis ventralis* on the wide concavities of the *basal tubera* and basioccipitals of *Anhanguera piscator* suggests a great mechanical advantage for ventral flexion of the head (Cleuren & De Vree 2000, Naish & Witton 2017).

The atlas-axis of *Anhanguera* and *Azhdarcho lancicollis* are morphologically similar to those of extant birds and crocodylians, but the pterosaur axis has more osteological correlates in common with extant birds (Mook 1921, Buchmann & Rodrigues 2024b). The wide insertion areas of the *transversospinalis cervicis*, *longissimus cervicis*, *flexor colli*, and *longus colli* are consistent with the extensive flexibility hypothesized for the articulation between occipital condyle and atlas-axis (Dzemski & Christian 2007, Taylor et al. 2009, Guinard et al. 2010, Krings et al. 2014, Böhmer et al. 2020). The extremely wide neural canal of the atlas-axis also supports the hypothesis of broad mobility, enabling freedom of movement of the spinal cord during cervical movements (Krings et al. 2014, 2017). The robust insertions of the *intercristales*, *interspinales*, and *longissimus cervicis* compared to the other muscles indicate their roles in the stability of this extremely mobile region, which is supported by the complexity of the joint between the occipital condyle and atlas-axis (Krings et al. 2014, 2017, Grytsyshina et al. 2016, Böhmer et al. 2020).

The laterally developed tubercles on the atlas-axis of *Anhanguera* and *Azhdarcho lancicollis* probably optimized the anchoring of the shorter bundles of the *longissimus capitis profundus* (Snively & Russell 2007, Boumans et al. 2015, Buchmann & Rodrigues 2024b). Our inference of a more caudal origin of the *splenius capitis* differs from that inferred for *Hatzegopteryx*, although the authors named the muscle as the homologous

epistropheo-capitis (Naish & Witton 2017). The extended hypapophyses seen in the atlas-axis provided a broad attachment site for the origins of the most cranial bundles of the *rectus capitis lateralis* and *rectus capitis ventralis*, which may have contributed to supporting broad ventral flexion and yaw of the head (Boumans et al. 2015, Böhmer et al. 2020).

The accumulation of muscles of the craniocervical system in the cranial half of the neck probably increased the weight of this region, which already supported the weight of a long skull in several pterosaurs (Vanden-Berge & Zweers 1993, Campos & Kellner 1997, Kellner & Tomida 2000, Bennett 2001, Kellner & Campos 2002, Dzemski & Christian 2007, Witton & Naish 2008, Pinheiro et al. 2011, Bantim et al. 2014, Naish & Witton 2017, Andres & Langston Jr. 2021, Beccari et al. 2021). However, the sinuous posture of the neck of pterosaurs could minimize stress in this region, as this orientation of the cervical series would provide the complementation of divergent tension and compression forces (Furet et al. 2018, Fasquelle et al. 2019, Buchmann & Rodrigues 2024a).

The *complexus*, *flexor colli*, *longissimus capitis profundus*, *rectus capitis lateralis*, and *rectus capitis ventralis* probably had their longest bundles originating in the tubercles or hypapophyses of the fifth or sixth cervical vertebra, as in extant archosaurs (Frey 1988, Snively & Russell 2007, Böhmer et al. 2020, Buchmann & Rodrigues 2024b). However, such length in pterosaurs represents bundles extending from the skull to mid-neck, whereas in extant birds the bundles do not exceed the first, ventrally concave cervical segment (Böhmer et al. 2020, Buchmann & Rodrigues 2024b). The lack of preservation of the sixth vertebra and the cranial portion of the seventh vertebra made it difficult to infer the origin of these five muscles in *Anhanguera piscator* (Kellner & Tomida 2000). However, the presence of developed tubercles and short hypapophyses in the sixth and seventh vertebrae of AMNH 22555 (*Anhanguera* sp.) supports our inferences, as the postcranial elements are very similar within that genus (Kellner & Tomida 2000).

The length of the muscles of the craniocervical system up to half the neck probably provided consolidation to the origins, which optimized skull movements (Cleuren & De Vree 2000, Snively & Russell 2007). Furthermore, the *complexus* and *rectus capitis ventralis* had the higher F_{pmax} of muscles in the neck of *Anhanguera piscator* and *Rhamphorhynchus muensteri* and the strongest among the craniocervical system of *Azhdarcho lacincollis*, which agrees with both muscles being mainly responsible for the pitching of the skull (Table II) (Burton 1974, Cleuren & De Vree 2000, Snively & Russell 2007). Similarly to birds, the *complexus* could also present intramuscular septa that would linearly increase muscular strength in pterosaurs, but we were unable to infer the unequivocal presence of these septa through osteological correlates (Buchmann & Rodrigues 2024b).

In all analyzed pterosaurs, the *longissimus capitis profundus* and *rectus capitis lateralis* probably exerted a force much smaller than those of the *rectus capitis ventralis* and *longissimus capitis superficialis* during ventral flexion and roll of the head, respectively, which may indicate that they only made additional efforts to make the movements faster and more elaborate (Table II) (Cleuren & De Vree 2000, Snively & Russell 2007).

The tall neural spine of the mid-cervical vertebrae of *Anhanguera* and *Rhamphorhynchus muensteri* provided broad areas of origin for the *transversospinalis capitis*, which added firmness to the muscle belly and imparted powerful dorsal flexion of the skull (Snively &

Russell 2007, Witton & Naish 2008, Böhmer et al. 2020). Furthermore, the developed neural spines are related to opposing the bending moment produced after ventral flexion of the neck and head, in which the lever arm of interspinous and supraspinous ligaments, and supraspinous muscles, represented by the height of the cervical vertebrae, would transmit the tension to the neural arch in response to the compression transmitted to the vertebral centra (Christian & Preuschoft 1996, Tambussi et al. 2012). The variation observed between the highest and proportionally lowest F_{pmax} of the *transversospinalis capitis* of *Rhamphorhynchus muensteri* and *Anhanguera piscator*, respectively, is probably related to their respective small and large volume of the *complexus*, which is the main muscle responsible for dorsal flexion of the skull (Snively & Russell 2007, Böhmer et al. 2020).

Despite the reduced neural spines in the mid-cervical vertebrae of *Azhdarcho lancicollis*, the presence of the *transversospinalis capitis* in azhdarchid pterosaurs has previously been proposed based on the height of the neural spines at the cranial and caudal ends of the neck (Witton & Naish 2008). Our muscle volume estimates indicate a slightly robust *transversospinalis capitis* along the neck in all analyzed pterosaurs, demonstrating that the attachment area should not be the only indication of muscle volume (Naish & Witton 2017). In addition, the variation in muscle volumes would have a linear effect on F_{pmax} estimates (Bishop et al. 2021).

The smaller area of muscular origin only indicates a reduction in its anchorage points in *Azhdarcho lancicollis*, which is consistent with the lower F_{pmax} for muscles that dorsoventrally flexioned the head compared to the muscles responsible for cervical pitching in this pterosaur (Table II) (Snively & Russell 2007, Cobley et al. 2013). Furthermore, segmented ligaments between neural spines could help restore the resting cervical position after ventral flexion of the skull of pterosaurs (Dimery et al. 1985, Gál 1993, Tsuihiji 2004, Buchmann & Rodrigues 2024a).

The broad attachment area of the insertions of the *transversospinalis cervicis* and *longus colli* in the preexapophyses and epipophyses enabled wide cervical pitching in the cranial half and middle of the neck, as in extant archosaurs (Burton 1974, Snively & Russell 2007, Boumans et al. 2015, Fronimos & Wilson 2017, Iijima & Kubo 2019, Böhmer et al. 2020, Buchmann & Rodrigues 2024b). The wide pitching in the cranial portion of the neck is also supported by the F_{pmax} found for the *transversospinalis cervicis* and *longus colli* (Table II). Furthermore, the larger dorsoventral amplitude agrees with the wide and long zygapophyses from the fourth to the sixth cervical vertebrae of pterosaurs, which increases the vertebral length and, consequently, the cervical lever arm in this region (Christian & Preuschoft 1996, Tambussi et al. 2012). Especially in *Azhdarcho lancicollis*, the F_{pmax} of the *transversospinalis cervicis* and *longus colli* were the greatest among all muscles and the zygapophyseal length of the mid-cervical vertebrae is accentuated, which indicates an optimization of the cervical pitching in relation to that performed by the skull (Table II) (Tambussi et al. 2012). The very elongated mid-cervical vertebrae of azhdarchid pterosaurs also contributed to the longer lever arm in this region, which generated greater torque to enhance dorsoventral flexion of the neck (Christian & Preuschoft 1996, Buchmann & Rodrigues 2024a).

Our reconstruction of a *transversospinalis cervicis* attached to the epipophyses agrees with previous inferences that the muscles responsible for dorsal flexion of the neck are attached to structures in the zygapophyses of azhdarchid

vertebrae (Herrel & De Vree 1999, Tsuihiji 2005, Snively & Russell 2007). The inferred length for the *transversospinalis cervicis* along the neck of *Rhamphorhynchus muensteri* is also supported by the presence of epipophyses in mid-cervical vertebrae (Wellnhofer 1975). The presence of the developed capitular process in *Rhamphorhynchus muensteri* indicates an additional area for broad attachments of the *longus colli* in the cranial half of the neck, as observed in extant crocodylians (Cleuren & De Vree 2000, Tsuihiji 2007, Snively & Russell 2007). Furthermore, the cervical ribs of *Rhamphorhynchus muensteri* could be attachment sites of intercostal muscles, such as the *iliocostalis capitis*, *iliocostalis cervicis*, and *intercostales externi*, as in *Caiman latirostris*, and the *inclusi*, as in birds (Frey 1988, Tsuihiji 2007, Figueiredo et al. 2016). However, the preservation of MGUH 1891.738 made it difficult to identify correlates that could support the presence of soft tissues between cervical ribs.

We named the muscle "*flexor colli*" here without specifying its lateral or medial arrangement, as we did not find evidence to support the presence of another flexor muscle belonging to the *iliocostalis* group, as seen in extant birds (Tsuihiji 2007). The insertions of the *flexor colli* suggest a function of ventral flexion of the cranial end of the neck, although the low F_{pmax} indicates that it primarily augmented movement performed by the *longus colli* (Snively & Russell 2007, Boumans et al. 2015, Böhmer et al. 2020).

Cervical yaw of the first half of the neck was probably accomplished through the contraction of the most cranial segments of the *longissimus cervicis*, which were inserted lateral to the neural arch of each vertebra (Snively & Russell 2007, Böhmer et al. 2020). However, the F_{pmax} found for the *longissimus cervicis* and the elongation of the vertebrae, the widening between the zygapophyses, and the narrowing of the neural canal from the fourth to the sixth vertebra indicate the limitation of lateral movement, which suggests that the cervical yaw and roll in the cranial half of the neck was restricted to the region closest to the skull (Zusi 1962, Burton 1974, Cleuren & De Vree 2000, Dzemski & Christian 2007, Snively & Russell 2007, Witton & Naish 2008, Krings et al. 2014, 2017, Molnar et al. 2015, Grytsyshina 2016, Vidal et al. 2020). The weak F_{pmax} attributed to the *longissimus cervicis* when compared to that observed for *longissimus capitis superficialis* (responsible for head yaw) can also be explained by the segmented arrangement, which indicates that the muscle exerted relatively low force but could be effective in stabilizing the neck laterally (Snively & Russell 2007).

We suggest that the origins of the *longissimus capitis superficialis* were fixed from the fifth cervical to the first dorsal vertebra in *Anhanguera piscator* due to the similarity of the muscle scar identified in the specimen AMNH 22555 (*Anhanguera* sp.).

Osteological correlates are more developed, mainly in the posterior cervical vertebrae, which gives more robustness to the muscular origins, as observed in extant archosaurs (Zweers et al. 1987, Chamero et al. 2014, Boumans et al. 2015, Iijima & Kubo 2019, Böhmer et al. 2020). The robustness of the bundles originating in the caudal half of the neck indicates that the *transversopinalis capitis*, *transversopinalis cervicis*, *longissimus capitis superficialis*, and *longus colli* were more stable in this region, which would promote consolidation for movement in the insertion bundles (Cleuren & De Vree 2000, Snively & Russell 2007). The robustness of the muscles in the caudal portion is also reflected in the F_{pmax} which, together with that great mechanical advantage, promoted optimized movements of

the skull and the neck (Seidel 1978, Frey 1988, Snively & Russell 2007, Naish & Witton 2017).

We observed that the insertions of *transversospinalis cervicis*, *longus colli*, and *longissimus cervicis* were restricted from the sixth to the eighth vertebra, which indicates that the cervical pitching and yaw movement were limited in this region. The great F_{pmax} of the *transversospinalis cervicis* and *longus colli* and the vertebral lever arm mainly in *Azhdarcho lancicollis* are consistent with the ability to pitch between the fifth and eighth cervical vertebrae and the repositioning of the neck after this movement, which suggests that the dorsoventral range began from the cervical vertebrae near the base of the neck (Seidel 1978, Frey 1988, Cleuren & De Vree 2000, Snively & Russell 2007).

The reduction in pitching potential in the cervical caudal end is consistent with the shortening of the vertebrae in the region, which reflects the shorter vertebral lever arm (Dzemski & Christian 2007). However, lengthening the intervertebral space would probably still allow for mild interarticular pitching (Zusi 1962, Haher et al. 1991, Selbie et al. 1993, Wintrich et al. 2019, Jones et al. 2021, Buchmann & Rodrigues 2024a). Furthermore, cervical dorsal flexion and the ability to keep the neck and skull suspended could still be optimized by robust segmented ligaments, mainly in the caudal half of the neck (Gál 1993, Dzemski & Christian 2007, Witton & Habib 2010, Buchmann & Rodrigues 2024a).

The attachments of the *longissimus cervicis* to broad transverse processes indicate that there were more robust muscle segments in the caudal half than in the cranial half of the neck, which could intensify cervical yaw between the fifth and eighth vertebrae (Snively & Russell 2007, Böhmer et al. 2020). The execution of wide lateral incursions in this region is consistent with the narrowing between the zygapophyses and the widening of the neural canal (Krings et al. 2014, 2017).

Segments of the *longissimus cervicis*, *interspinales*, and *intercristales* muscles that attached to adjacent vertebrae throughout the neck provided resistance and stabilization in response to the compressions and tensions that occur alternately during the pitching of the neck (Carlson 1978, Christian & Preuschoft 1996, Witton & Habib 2010, Tambussi et al. 2012, Averianov 2013, Cobley et al. 2013, Gutzwiller et al. 2013, Molnar et al. 2014, Moore 2020). Furthermore, the larger volume of these muscles close to the posterior cervical vertebrae indicates that such compressions and tensions were intensified in this region, possibly due to the long distance from the base of the neck to the skull (Cobley et al. 2013, Molnar et al. 2014).

The presence of the *interspinales* throughout the neck of pterosaurs resembles that observed in extant crocodylians and differs from birds, in which the muscles are restricted to the most cranial vertebrae of the neck (Frey 1988, Tsuihiji 2005, Buchmann & Rodrigues 2024b). The presence of tall neural spines on all cervical vertebrae of *Anhanguera* and *Rhamphorhynchus muensteri* allowed for more robust *interspinales*, which contributed to intervertebral stabilization across the entire cervical range (Carlson 1978, Snively & Russell 2007). The *interspinales* and *intercristales* presented the lowest F_{pmax} among the muscles, probably due to their main function as cervical stabilizers (Table II) (Carlson 1978, Snively & Russell 2007). The *intercristales* are still responsible for intervertebral dorsoventral flexion between the mid-cervical vertebrae, however, their contraction would probably result in a slight pitching (Snively & Russell 2007).

According to the musculature of extant archosaurs, most cervical muscles originate through aponeuroses, which increases the area of attachment and makes it more stable

compared to tendons (McGowan 1979, 1986, Bryant & Seymour 1990, Snively & Russell 2007). However, five neck muscles are also inserted via aponeuroses, which may also be related to the strength provided by this attachment (Bryant & Seymour 1990, Snively & Russell 2007). Aponeurotic attachments were associated with the rough surface of the bone cortex at the origins of the *longissimus capitis superficialis*, *longissimus capitis profundus*, *flexor colli*, *rectus capitis lateralis*, and *rectus capitis ventralis* and at the insertions of the *flexor colli*, *longissimus cervicis*, and *longus colli*, which may indicate a relationship between this type of attachment and the impression produced on the bone surface (McGowan 1979, 1986, Bryant & Seymour 1990). However, it should be noted that the *complexus*, *transversospinalis cervicis*, and *intercristales* probably originated from aponeuroses in the region between the epipophyses and the neural spine, which have a smooth surface (Snively & Russell 2007).

The fleshy attachments that are common between the muscles of the craniocervical system probably conferred strength, as this type of attachment is even more robust than aponeuroses (Snively & Russell 2007). The origins and insertions of the *interspinales* agree with the robustness conferred by fleshy attachments, as they increase stability between the neural spines (Carlson 1978). Muscle scars were often found on bone surfaces related to fleshy attachments, which was expected due to the strength imparted by this type of attachment (McGowan 1979, 1986, Nicholls & Russell 1985, Bryant & Seymour 1990).

Lastly, tendon attachments have seldom been inferred for pterosaur neck muscles as they are less common in the cervical musculature of extant archosaurs (Snively & Russell 2007, Figueiredo et al. 2016). They were more numerous among the muscle insertions responsible for cervical pitching, which is consistent with the increased mobility and flexibility capacity conferred by this type of attachment (McGowan 1979, 1986, Bryant & Seymour 1990, Snively & Russell 2007).

Implications for pterosaur life habits

There are still many inconsistencies regarding the foraging habits of pterosaurs (Wellnhofer 1975, Kellner & Tomida 2000, Humphries et al. 2007, Frey & Tischlinger 2012). The morphology of the forelimbs and the lack of developed claws demonstrate that their head was responsible for collecting food, thus the advantages of a long and mobile neck (Witton & Naish 2008, Marek et al. 2021, Marek 2023). The foods they consumed can be observed directly in the rare instances of bromalite preservation or, more often, are inferred through comparative anatomy, analyzing fossils that are present in the same geological units where they are preserved, or by physicochemical analyses such as using stable isotopes (Wellnhofer 1975, Kellner & Tomida 2000, Witton & Naish 2008, 2015, Hone et al. 2015, Bestwick et al. 2018, Jiang et al. 2022).

Rhamphorhynchus muensteri is one of the few pterosaurs with preserved stomach contents, being well-known to feed on fish, and further evidence suggests that at least occasionally it also preyed on squid (Hone et al. 2015, Hoffmann et al. 2020). Furthermore, the specialized dentition, association with fish in the fossil record, and the results of isotopic and biomechanical analyses indicate that both rhamphorhynchids and anhanguerids were piscivores, in the broader sense that encompasses fish and other soft aquatic animals (Wellnhofer 1975, Padian 2008, Amiot et al. 2010, Tütken & Hone 2010, Frey & Tischlinger 2012, Veldmeijer et al. 2012, Wang et al. 2012, Hone et al. 2013, 2015, Bestwick et al. 2018, Henderson 2018, Pêgas et al. 2020).

The capture method of pterosaurs with aquatic foraging probably varied, given the different adaptations presented by the species (Wellnhofer 1991, Kellner & Tomida 2000, Kellner & Campos 2002). Anhanguerids are interpreted as aerial piscivores because their wings have adequate proportions for dynamic flights, as in extant seabirds (Witton & Habib 2010). One of the hypotheses raised for the capture of aquatic prey is the skimming habit, observed in Rynchopidae birds, which forage in calm and shallow waters, and proposed for the pterosaur *Thalassodromeus sethi* (Zusi 1962, Kellner & Campos 2002). However, the execution of this habit seems unlikely for *Anhanguera*, due to the high energy expenditure that would be required for an animal of this weight (Humphries et al. 2007). Furthermore, pterosaurs apparently do not have skull adaptations necessary for skimming, which would also exclude the possibility of lighter animals such as *Rhamphorhynchus* performing this habit (Humphries et al. 2007). Furthermore, the cranial half of the pterosaur neck is not segmented as in *Rynchops*, which makes it difficult to resist the continuous drag generated during possible skimming (Humphries et al. 2007, Buchmann & Rodrigues 2024a). Other fishing methods, on the banks or at the water surface, would require low energy costs and were probably favored by rhamphorhynchids and anhanguerids in capturing fish and other prey (Frey & Tischlinger 2012, Habib 2015).

Skimming is also unlikely for *Azhdarcho* due to the proposed flight, high energy cost, cervical inflexibility, and lack of necessary morphological adaptations in the skull (Humphries et al. 2007). An earlier hypothesis proposed that the long neck of azhdarchids was associated with reaching deeper in a likely fishing habit (Nesov 1984), but more recent proposals suggest that the long rostrum of the azhdarchid skull resembles that of birds that forage in a terrestrial environment, and thus, they have been hypothesized to be terrestrial generalists (Witton & Naish 2008, 2015). Azhdarchids include both large and giant taxa, a variation that indicates that different species may have fed on smaller or larger prey (Carroll et al. 2013, Witton & Naish 2015, Naish & Witton 2017), and their diet could have been supplemented with the consumption of fruits and carrion (Witton & Naish 2008). *Azhdarcho lancicollis* probably limited its feeding to small foods that would not require much bite force, considering its gracile jaws and cervical elements (Witton & Naish 2008, 2015, Averianov 2010, Naish & Witton 2017).

The muscles inferred here indicate broad mobility of the head and neck in the analyzed pterosaurs, although the greatest range of motion performed during foraging was more developed from the head to the middle of the neck (Dzemski & Christian 2007, Cobley et al. 2013, Molnar et al. 2015, Boumans et al. 2015, Böhmer et al. 2020). The strongly marked scars on the occipital of *Anhanguera piscator* indicate that the pitching, yaw, and rolling capabilities of the skull were extensive, which is consistent with the vast cranial flexibility required for this pterosaur's underwater foraging (Weimerskirch et al. 2013, Gheler-Costa et al. 2018). Furthermore, the shape of the rostral crest of *Anhanguera* could be advantageous in stabilizing the beak during food capture in the water (Veldmeijer et al. 2007).

According to the F_{pmax} presented by the muscles, the main difference between the analyzed pterosaurs is the excellent capacity for pitching of the skull of both piscivores and the optimization for cervical pitching in *Azhdarcho lancicollis* (Table II). This difference in the cranial or cervical pitching is probably related to the posture of their neck in rest position (*sensu* Buchmann & Rodrigues 2024a). *Anhanguera piscator* and *Rhamphorhynchus*

muensteri probably maintained their necks more horizontally, which allowed the head to remain closer to the ground, while *Azhdarcho lancicollis* exhibited a more vertical cervical posture, which gave the head a higher position in relation to the ground (Buchmann & Rodrigues 2024a).

The great F_{pmax} of the *rectus capitis ventralis* and *complexus* of *Anhanguera* and *Rhamphorhynchus*, both piscivorous pterosaurs, would project the rostrum quickly towards the water surface and reposition it for a new attack with the same agility (Phalan et al. 2007, Gheler-Costa et al. 2018). Similarly, the extremely strong *longus colli* and *transversospinalis cervicis* of *Azhdarcho lancicollis* would allow rapid dorsoventral lunges of the neck to capture small, mobile prey in a terrestrial environment (Naish & Witton 2017). Furthermore, the long skulls known for azhdarchids could be flexed ventrally, which would contribute to reduce the distance between the head and the ground (Witton & Naish 2008).

The presence of a thinner *longissimus capitis profundus* and *flexor colli* would ensure that the flexion of the skull and neck varied in more axes, which would contribute to the versatility of movements in both foraging strategies (Phalan et al. 2007, Gheler-Costa et al. 2018). Furthermore, the position of the *longissimus capitis profundus* and *flexor colli* indicates that both could stabilize the ventral flexion movement performed by the *rectus capitis ventralis* and *longus colli*, respectively, which would allow pterosaurs to keep the skull facing ventrally during foraging, to search for prey (Phalan et al. 2007, Weimerskirch et al. 2013, Gheler-Costa et al. 2018).

In *Azhdarcho lancicollis*, the force produced by powerful muscles responsible for dorsal flexion of the head and neck would contribute to tearing off parts of fresh prey or carrion, as observed in extant carnivorous and scavenging birds (Redford & Peters 1986, Houston 1988, Böhmer et al. 2020). The high F_{pmax} of the *transversospinalis capitis* of *Rhamphorhynchus muensteri* and of the *complexus* of *Anhanguera piscator* indicates possible capabilities for rapid retraction of the skull and sudden lateral movements of the head, respectively, which resembles habits for rapid ingestion or slaughter of prey done by extant archosaurs (Weimerskirch et al. 2013, Gheler-Costa et al. 2018). The rapid head retraction hypothesis is also in line with the agile bite previously inferred for anhanguerids (Pêgas et al. 2020). Even with those differences, the great F_{pmax} of the *transversospinalis capitis*, *complexus*, *splenius capitis*, and *transversospinalis cervicis* optimized the dorsal flexion of the skull and neck in *Anhanguera piscator* and *Rhamphorhynchus muensteri* (Table II). The robustness of these muscles in these pterosaurs is compatible with the ability to quickly submerge the head during the aquatic foraging inferred for them (Vidal et al. 1986, Kellner & Tomida 2000, Habib 2015, Vidal et al. 2020).

The robust muscles located dorsally to the cervical series in the pterosaurs analyzed could control dorsal flexion throughout the range of elevation of the head and neck after prey capture (Dzemski & Christian 2007). In this case, control of the cervical posture would be optimized by the presence of segmented ligaments arranged between the cervical vertebrae (Dimery et al. 1985, Ponseti 1995, Tsuihiji 2004, Dzemski & Christian 2007, Buchmann & Rodrigues 2024a). The control of total dorsal flexion would also be important for pterosaurs to maintain an alert position, in which keeping the neck fully extended dorsally would allow a more comprehensive view of the environment (Dzemski & Christian 2007).

The high F_{pmax} of the *longissimus capitis superficialis* indicates that the skull was capable of wide yaw and roll, which confers

more dexterity to the movement in a possible hunting habit (Snively & Russell 2007, Böhmer et al. 2020). According to the F_{pmax}, the lateral movement of the skull was as strong as the pitching in *Azhdarcho lancicollis*, which indicates that cranial maneuverability was a skill in the foraging habit of this pterosaur (Naish & Witton 2017). Carrying out wide lateral excursions promoted by the *longissimus cervicis* between the sixth and eighth cervical vertebrae could completely yaw the cranial portion of the neck, which would allow the head to be positioned laterally to encompass a view of the environment (Snively & Russell 2007, Böhmer et al. 2020).

The remarkable stabilization capacity of the cervical vertebral column promoted by the contraction of the segmented muscles would have been useful during rapid lunges of the neck to capture prey (Carlson 1978, Dzemski & Christian 2007). This stabilization could be intensified by the action of the articular ligaments that bordered the vertebral joints of the neck of pterosaurs (Ponseti 1995, Dzemski & Christian 2007, Buchmann & Rodrigues 2024a).

The presence of the *intercristales*, *interspinales* and *longissimus cervicis* throughout the neck could still provide intrinsic stability in different postures throughout the cervical range of movements, which is important for establishing different positions of the head during varied habits (Zweers et al. 1994, Marek et al. 2021, Marek 2023). Furthermore, the stiffening of these segmented muscles could reduce the compressions and tensions transmitted between the vertebral joints, which would minimize the effects of additional weight of prey captured during the repositioning of the pterosaur neck to the position at rest (Christian & Preuschoft 1996, Tambussi et al. 2012, Buchmann & Rodrigues 2024a). The extremely low F_{pmax} observed for *intercristales* and *interspinales* indicates that both could perform functions that are not necessarily muscular, such as sensory functions.

The values obtained for the muscular forces represent an exact solution only in the mathematical formula. In practice, we believe that it is an approximate value, since our analysis was carried out based on estimated proportions in phylogenetically close extant animals. However, our objective was not only to obtain an approximate value for the forces exerted on the neck, but also to compare the performance of each cervical muscle in a pterosaur. Therefore, we must consider that all movements inferred by the predicted capacity of the muscles may not represent the habits performed by animals in life (Jones et al. 2021).

CONCLUSIONS

Based on the osteological correlates present in the cervical vertebrae of the analyzed pterosaurs, we inferred the presence of thirteen cervical muscles, of which only the *longissimus capitis superficialis* did not have an inference level I by the EPB criteria. Six of them probably had their length limited from the head to about the middle of the cervical series, enabling complex movements and a mobile head, but likely subjected the cranial cervical region to more stress. Aponeurotic attachments on the vertebrae and fleshy muscular insertions on the skull were more common among the cervical muscles, which would confer robustness to the muscular attachments and agree with the association of muscles with scars and rough areas in the bone cortex.

The proportion we followed defined the neck muscle volume through the points at which the bundles would form the maximum thickness of each muscle, as we observed in the cervical muscles of extant birds. We inferred that the volume filled by the epaxial muscles was

greater than that of the hypaxials, but the most voluminous muscle among all those inferred was the *longus colli*, a hypaxial muscle.

We observed that *Anhanguera* and *Rhamphorhynchus muensteri* could have an optimization in the ventral flexion of the head, while in *Azhdarhco lancicollis* this flexion was improved in the neck. Such specializations in the ventral flexion of the skull and neck indicate a relationship with the cervical resting posture of pterosaurs. On the other hand, the considerably low F_{pmax} of the *longissimus capitis profundus* and *flexor colli* may represent additional functions beyond ventral flexion of the skull and neck, such as expanding the range in more axes or providing movement stabilization. In dorsal flexion, the robustness of the *splenius capitis* would also guarantee greater control over the head elevation in all the analyzed pterosaurs.

Unilateral flexion of the strong *complexus* would drive lateral motions of the skull, which, together with a moderately forceful *longissimus capitis superficialis*, would actuate a laterally movable head. According to the insertion sites, the contraction of the *longissimus capitis superficialis* and *rectus capitis lateralis* would also promote skull roll, which, according to F_{pmax}, would be relatively less extensive than the lateral movements. Unlike with skull motions, the cervical lurch was more discrete, and could be wider only in the middle of the neck. The low F_{pmax} of *interspinales* and *intercristales* indicates that both had a limited role in cervical stabilization and proprioception, which is supported by both presenting an effective morphology in transmitting position and orientation.

The inferred musculature corroborates the possible surface fishing foraging habits of *Anhanguera* and *Rhamphorhynchus muensteri* and the capture of small terrestrial prey by *Azhdarcho lancicollis*. However, estimates of cervical motion should be inferred with caution, as many of the properties that influence mechanics can be difficult to observe in pterosaur fossils. Other factors must also be considered for the execution of the movements we discuss, such as vertebral bone resistance to loads generated by soft tissues and reaction forces from prey.

Acknowlegments

We thank Niels Bonde (Zoological Museum, Denmark), Maria Eduarda Castro Leal (Zoological Museum, Denmark), Michael Storey (Zoological Museum, Denmark), Alexander Averianov (Zoological Institute of the Russian Academy of Sciences, Russia), Takanobu Tsuihiji (National Museum of Nature and Science, Japan), Makoto Manabe (National Museum of Nature and Science, Japan), Chisako Sakata (National Museum of Nature and Science, Japan), who scanned the specimens and gently shared the data with us. We would also like to thank Carl Mehling (American Museum of Natural History) and Roger Benson (American Museum of Natural History) for collection access. We would like to thank Rodrigo Pêgas for their help in photographing the specimens. We are also grateful to the coordinators and staff of the Institute for the Research and Rehabilitation of Marine Animals (Instituto de Pesquisa e Reabilitação de Animais Marinhos - IPRAM) (Cariacica, Brazil), the State Institute of Environment and Water Resources (Instituto Estadual de Meio Ambiente e Recursos Hídricos - IEMA), and the Caiman Project (Vitória, Brazil). We thank Alexandre Liparini (Universidade Federal de Minas Gerais), Felipe Montefeltro (Universidade Estadual Paulista), Fabiana Costa (Universidade Federal do ABC), and Felipe Pinheiro (Universidade Federal do Pampa) for comments on an earlier version of this manuscript. Finally, we thank Dr. Eric Snively and the anonymous reviewers for their valuable contributions in reviewing this manuscript. This study was partially funded by Coordenação de Aperfeiçoamento de Pessoal de Nível Superior – Brazil (CAPES) – Finance Code 001 (scholarship to RB); by Conselho Nacional de Desenvolvimento Científico e Tecnológico (CNPq), Brazil, project grant #314260/2021-8 to TR; and Fundação de Amparo à Pesquisa e Inovação do Espírito Santo (FAPES), Brazil, project grant #705/2022 to TR and scholarship to RB. The funders had no role in study design, data collection and analysis, decision to publish, or preparation of the manuscript.

REFERENCES

ALLEN V, PAXTON H & HUTCHINSON. 2009. Variation in center of mass estimates for extant sauropsids and its importance for reconstructing inertial properties of extinct archosaurs. Anat Rec 292: 1442-1461.

AMIOT R ET AL. 2010. Oxygen and carbon isotope compositions of middle Cretaceuos vertebrates from North Africa and Brazil: ecological and environmental significance. Palaeogeogr Palaeocl 297: 439-451.

ANDRES B & LANGSTON-JR W. 2021. Morphology and taxonomy of *Quetzalcoatlus* Lawson 1975 (Pterodactyloidea: Azhdarchoidea). J Vertebr Paleontol 41: 46-202.

AVERIANOV AO. 2010. The osteology of *Azhdarcho lancicollis* (Nessov, 1984) (Pterosauria, Azhdarchidae) from the late Cretaceous of Uzbekistan. Proc Zool Inst RAS 314: 264-317.

AVERIANOV AO. 2013. Reconstruction of the neck of *Azhdarcho lancicollis* and lifestyle of azhdarchids (Pterosauria, Azhdarchidae). Paleontol J 47: 203-209.

BANTIM RAM, SARAIVA AAF, OLIVEIRA GR & SAYÃO JM. 2014. A new toothed pterosaur (Pterodactyloidea: Anhangueridae) from the Early Cretaceous Romualdo Formation, NE Brazil. Zootaxa 3869(3): 201-223.

BATES KT & SCHACHNER ER. 2012. Disparity and convergence in bipedal archosaur locomotion. J R Soc Interface 9: 1339-1353.

BAUMEL JJ & WITMER LM. 1993. Osteologia. In: Baumel JJ, King AS, Breazile JC, Evans HE & Vanden Berge JC (Eds), Handbook of avian anatomy: *Nomina anatomica avium*, Cambridge: Nuttal Ornihtological Club, p. 45-132.

BECCARI V, PINHEIRO FL, NUNES I, ANELLI LE, MATEUS O & COSTA FR. 2021. Osteology of an exceptionally well-preserved tapejarid skeleton from Brazil: Revealing the anatomy of a curious pterodactyloid clade. PLoS ONE 16(8): e0254789.

BENNETT SC. 2001. The osteology and functional morphology of the Late Cretaceous pterosaur *Pteranodon*. Part I General Description of Osteology. Paleontogr Abt A 260: 1-112.

BENNETT SC. 2003. Morphological evolution of the pectoral girdle of pterosaurs: myology and function. Geol Soc Spec Publ 217: 191-125.

BESTWICK J, UNWIN DM, BUTLER RJ, HENDERSON DM & PURNELL MA. 2018. Pterosaur dietary hypotheses: a review of ideas and approaches. Biol Rev 93: 2021-2048.

BLENDER DEVELOPMENT TEAM. 2019. Blender (Version 4.0) [Computer software]. https://www.blender.org.

BISHOP PJ, CUFF AR & HUTCHINSON JR. 2021. How to build a dinosaur: Musculoskeletal modeling and simulation of locomotor biomechanics in extinct animals. Paleobiology 47(1): 1-38.

BOAS JEV. 1929. Biologisch-anatomische Studien über den Hals der Vögel. Kongl. Danske Vidensk. Selsk. Skrifter, Naturvidensk. Math (Ser. 9) 1: 105-222.

BÖHMER C, PREVOTEAU J, DURIEZ O & ABOURACHID A. 2020. Gulper, ripper and scrapper: anatomy of the neck in three species of vultures. J Anat 236: 701-723.

BONDE N & CHRISTIANSEN P. 2003. The detailed anatomy of *Rhamphorhynchus*: axial pneumaticity and its implications. Geol Soc Spec Publ 217: 217-232.

BOUMANS MLLM, KRINGS M & WAGNER H. 2015. Muscular arrangement and muscle attachment sites in the cervical region of the American barn owl (*Tyto furcata pratincole*). PLoS ONE 10: e0134272.

BOYER DM, GUNNELL GF, KAUFMAN S & MCGEARY TM. 2017. Morphosource: archiving and sharing 3-D digital specimen data. Paleontol Soc Papers 22: 157-181.

BRAUN EL & KIMBALL RT. 2021. Data types and the phylogeny of Neoaves. Birds 2(1):10.3390/birds2010001.

BRYANT HN & SEYMOUR KL. 1990. Observations and comments on the reliability of muscle reconstruction in fossil vertebrates. J Morphol 206: 109-117.

BUCHMANN R & RODRIGUES T. 2024a. Arthrological reconstructions of the pterosaur neck and their implications for the cervical position at rest. PeerJ 12: e16884.

BUCHMANN R & RODRIGUES T. 2024b. Cervical anatomy and its relation to foraging habits in aquatic birds (Aves: Neornithes: Neoaves). Anat Rec 307(10): 3204-3229.

BUCHMANN R, RODRIGUES T, POLEGARIO S & KELLNER AWA. 2018. New information on the postcranial skeleton of the Thalassodrominae (Pterosauria, Pterodactyloidea, Tapejaridae). Hist Biol 30: 1139-1149.

BURTON PJK. 1974. Feeding and the feeding apparatus in waders: a study of anatomy and adaptations in the Charadrii. London: British Museum Press, 719 p.

CAMPOS DA & KELLNER AWA. 1997. Short note on the first occurrence of Tapejaridae in the Crato Member (Aptian), Santana Formation, Araripe Basin, Northeast Brazil. An Acad Bras Cienc 69(1): 83-87.

CARLSON H. 1978. Morphology and contraction properties of cat lumbar back muscles. Acta Physiol Scand 103: 180-197.

CARROLL NR, POUST AW & VARRICCHIO DJ. 2013. A third azhdarchid pterosaur from the Two Medicine Formation (Campanian) of Montana. In: Sayão JM, Costa FR, Bantim RAM & Kellner AWA (Eds), International Symposium on pterosaurs, Rio Ptero 2013, Rio de Janeiro: Universidade Federal do Rio de Janeiro, p. 40-42.

CHAMERO B, BUSCALIONI AD, MARUGÁN-LOBÓN J & SARRIS I. 2014. 3D geometry and quantitative variation of the cervico-thoracic region in Crocodylia. Anat Rec 297: 1278-1291.

CHRISTIAN A & PREUSCHOFT H. 1996. Deducing the body posture of extinct large vertebrates from the shape of the vertebral column. Palaeontology 39(4): 801-812.

CLEUREN J & DE VREE F. 2000. Feeding in crocodilians. In: Schwenk K (Ed), Feeding: form, function, and evolution in tetrapod vertebrates, San Diego: Academic Press, p. 337-358.

COBLEY MJ, RAYFIELD EJ & BARRETT PM. 2013. Inter-Vertebral Flexibility of the Ostrich Neck: Implications for Estimating Sauropod Neck Flexibility. PLoS ONE 8(8): e72187.

COX SM, EASTON KL, LEAR MC, MARSH RL, DELP SL & RUBENSON J. 2019. The interaction of compliance and activation on the force-length operating range and force generating capacity of skeletal muscle: a computational study using a guinea fowl musculoskeletal model. Integr Comp Biol 1: obz022.

DAVIES MNO & GREEN PR. 1994. Perception and motor control in birds. An ecological approach. Berlin: Springer, 364 p.

DELP SL, ANDERSON FC, ARNOLD AS, LOAN P, HABIB A, JOHN CT, GUENDELMAN E & THELEN DG. 2007. OpenSim: open-source software to create and analyze dynamic simulations of movement. IEEE T Bio-med Eng 54: 1940-1950.

DIMERY NJ, ALEXANDER RM & DEYST KA. 1985. Mechanics of the *ligamentum nuchae* of some artiodactyls. J Zoo 206(3): 341-351.

DZEMSKI G & CHRISTIAN A. 2007. Flexibility along the neck of the ostrich (*Struthio camelus*) and consequences for the reconstruction of dinosaurs with extreme neck length. J Morphol 268: 701-714.

ECK K, ELGIN RA & FREY E. 2011. On the osteology of *Tapejara wellnhoferi* Kellner 1989 and the first occurrence of a multiple specimen assemblage from the Santana Formation, Araripe Basin, NE-Brazil. Swiss J Palaeontol 130: 277-296.

ELGIN RA & FREY E. 2011. A new azhdarchoid pterosaur from Cenomanian (Late Cretaceous) of Lebanon. Swiss J Geosci 104: 21-33.

FASQUELLE B, FURET M, CHEVALLEREAU C & WENGER P. 2019. Dynamic modeling and control of a tensegrity manipulator mimicking a bird neck. Mech Mach Sci 73: 2087-2097.

FIGUEIREDO S, ARAÚJO L, FERRAZ R & ARAÚJO E. 2016. Bases ósseas e musculares do corte comercial de pescoço de jacaré-do-pantanal (*Caiman yacare* Daudin, 1802). Pesq Vert Bras 36(2): 94-102.

FREY E. 1988. Anatomie des Korperstammes von *Alligator mississippiensis* Daudin. Stuttgarter Beitrage zur Naturkunde 424: 1-106.

FREY E & TISCHLINGER H. 2012. The Late Jurassic pterosaur *Rhamphorhynchus*, a frequent victim of the ganoid fish *Aspidorhynchus*? PLoS ONE 7(3): e31945.

FRONIMOS JA & WILSON JA. 2017. Concavo-convex intercentral joints stabilize the vertebral column in sauropod dinosaurs and crocodylians. Ameghiniana 54(2): 151-176.

FURET M, VAN RIESEN A, CHEVALLEREAU C & WENGER P. 2018. Optimal design of tensegrity mechanisms used in a bird neck model. Mech Mach Sci 59: 365-375.

GÁL JM. 1993. Mammalian spinal biomechanics 2: intervertebral lesion experiments and mechanisms of bending resistance. J Exp Biol 174: 281-297.

GHELER-COSTA C, COMIN FH, GILLI LC & VERDADE LM. 2018. Foraging behavior of Brazilian cormorant *Nannopterum brasilianus* (Suliformes: Phalacrocoracidae). Zoologia 35: e14664.

GRYTSYSHINA EE, KUZNETSOV AN & PANYUTINA AA. 2016. Kinematic constituents of the extreme head turn of *Strix aluco* estimated by means of CT-scanning. Dokl Biol Sciences 466: 24-27.

GUINARD G, MARCHAND D, COURANT F, GAUTHIER-CLERC M & LE BOHEC C. 2010 Morphology, ontogenesis and mechanics of cervical vertebrae in four species of penguins (Aves: Sphenicidae). Polar Biol 33: 807-822.

GUTZWILLER SC, SU A & O'CONNOR PM. 2013. Postcranial pneumaticity and bone structure in two clades of neognath birds. Anat Rec 296: 867-876.

HABIB MB. 2015. Size limits of marine pterosaurs and energetic considerations of plunge versus pluck feeding. In: The 5th International Symposium on Pterosaurs, Portsmouth. University of Portsmouth.

HABIB MB & GODFREY S. 2010. On the hypertrophied opisthotic processes in *Dsungaripterus weii* Young (Pterodactyloidea, Pterosauria). Acta Geoscientica Sinica 31: 26.

HAHER TR, BERGMAN M, O'BRIEN M, FELMLY WT, CHOUEKA J, WELIN D, CHOW G & VASSILIOU A. 1991. The effect of the three columns of the spine on the instantaneous axis rotation in flexion and extension. Spine 16(8): 12-18.

HENDERSON DM. 2018. Using three-dimensional, digital models of pterosaur skulls for the investigation of their relative bite forces and feeding styles. Geol Soc Spec Publ 455: 25-44.

HERREL A & DE VREE F. 1999. The cervical musculature in helodermatid lizards. Belgian J Zool 129: 175-186.

HOFFMANN R, BESTWICK J, BERNDT G, BERNDT R, FUCHS D & KLUG C. 2020. Pterosaurs ate soft-bodied cephalopods (Coleoidea). Sci Rep 10: 1230.

HONE D, HENDERSON DM, THERRIEN F & HABIB MB. 2015. A specimen of *Rhamphorhynchus* with soft tissue preservation, stomach contents and a putative coprolite. PeerJ 3: e1191.

HONE DWE, HABIB MB & LAMANNA MC. 2013. An annotated and illustrated catalogue of Solnhofen (Upper Jurassic, Germany) pterosaur specimens at Carnegie Museum of Natural History. Ann Carnegie Mus 82: 165-191.

HOUSTON DC. 1988. Competition for food between Neotropical vultures in forest. Ibis 130: 402-417.

HUMPHRIES S, BOSNER RHC, WITTON MP & MARTILL DM. 2007. Did pterosaurs feed by skimming? Physical modelling and anatomical evaluation of an unsual feeding method. PLoS BIOL 5: 1647-1655.

HUTCHINSON JR, ANDERSON FC, BLEMKER SS & DELP SL. 2005. Analysis of hindlimb muscle moment arms in *Tyrannosaurus rex* using a three-dimensional musculoskeletal computer model: implications for stance, gait and speed. Paleobiology 31: 676-701.

HUTCHINSON JR, MILLER CE, FRITSCH G & HILDEBRANDT T. 2008. The anatomical foundation for multidisciplinary studies of animal limb function: examples from dinosaur and elephant limb imaging studies. In: Endo H & Frey R (Eds), Anatomical imaging: towards a new morphology, Tokyo: Springer, p. 23-38.

HUTCHINSON JR, RANKIN JW, RUBENSON J, ROSENBLUTH KH, SISTON RA & DELP SL. 2015. Musculoskeletal modeling of an ostrich (*Struthio camelus*) pelvic limb: influence of limb orientation of muscular capacity during locomotion. PeerJ 3: e1001.

IIJIMA M & KUBO T. 2019. Comparative morphology of presacral vertebrae in extant crocodylians: taxonomic, functional and ecological implications. Zoo J Linn Soc-Lond 186: 1006-1025.

JIANG S, WANG X, ZHENG X, CHENG X, WANG X, WEI G & KELLNER AWA. 2022. Two emetolite-pterosaur associations from the Late Jurassic of China: showing the first evidence for antiperistalsis in pterosaurs. Phil Trans R Soc B 377: 20210043.

JONES KE, BROCKLEHURST RJ & PIERCE SE. 2021. AutoBend: An automated approach for estimating intervertebral joint function from bone-only digital models. Integr Organismal Biol 3: obab026.

KELLNER AWA & CAMPOS DA. 2002. The function of the cranial crest and jaw of a unique pterosaur from the Early Cretaceous of Brazil. Science 297: 389-392.

KELLNER AWA & LANGSTON-JR W. 1996. Cranial remains of *Quetzalcoatlus* (Pterosauria, Azhdarchidae) from Late Cretaceous sediments of Big Bend National Park, Texas. J Vertebr Paleontol 16: 222-231.

KELLNER AWA & TOMIDA Y. 2000. Description of a new species of Anhangueridae (Pterodactyloidea) with comments on the pterosaur fauna from the Santana Formation (Aptian-Albian), Northeastern Brazil. Tokyo: National Science Museum, Monographs, 135 p.

KRINGS M, NYAKATURA JA, BOUMANS MLLM, FISCHER MS & WAGNER H. 2017. Barn owls maximize head rotations by a combination of yawing and rolling in functionally diverse regions of the neck. J Anat 231: 12-22.

KRINGS M, NYAKATURA JA, FISCHER MS & WAGNER H. 2014. The cervical spine of the American barn owl (*Tyto furcata pratincola*): I. Anatomy of the vertebrae and regionalization in their S-shaped arrangement. PLoS ONE 9(3): e91653.

KRUUK H. 1967. Competition for food between vultures in East Africa. Ardea 55: 172-193.

KUHL H, FRANKL-VILCHES C, BAKKER A, MAYR G, NIKOLAUS G, BOERNO ST, KLAGES S, TIMMERMANN B & GAHR M. 2021. An unbiased molecular approach using 3' – UTRs resolves the avian family – level tree of life. Mol Biol Evol 38(1): 108-127.

MACAULAY S, HUTCHINSON JR & BATES KT. 2017. A quantitative evaluation of physical and digital approaches to centre of mass estimation. J Anat 231: 758-775.

MAREK RD. 2023. A surrogate forelimb: evolution, function and development of the avian cervical spine. J Morphol 284: e21638.

MAREK RD, FALKINGHAM PL, BENSON RBJ, GARDINER JD, MADDOX TW & BATES KT. 2021. Evolutionary versatility of the avian neck. P R Soc B 288: 20203150.

MCGOWAN C. 1979. The hind limb musculature of the Brown kiwi, *Apteryx australis mantelli*. J Morphol 160: 33-74.

MCGOWAN C. 1986. The wing musculature of the Weka (*Gallirallus australis*), a flightless rail endemic to New Zealand. J Zool Soc Lond 210: 305-346.

MOLNAR JL, PIERCE SE, BHULLAR BAS, TURNER AH & HUTCHINSON JR. 2015. Morphological and functional changes in the vertebral column with increasing aquatic adaptation in crocodylomorphs. Roy Soc Open Sci 2: 150439.

MOLNAR JL, PIERCE SE & HUTCHINSON JR. 2014. An experimental and morphometric test of the relationship between vertebral morphology and joint stiffness in Nile crocodiles (*Crocodylus niloticus*). J Exp Biol 217: 758-768.

MOOK CC. 1921. Notes on the postcranial skeleton in the Crocodilia. B Am Mus Nat Hist 44: 67-100.

MOORE AJ. 2020. Vertebral pneumaticity is correlated with serial variation in vertebral shape in storks. J Anat 238: 615-625.

MULLER J, SCHEYER TM, HEAD JJ, BARRETT PM, WERNEBURG I, ERICSON PGP, POL D & SÁNCHEZ-VILLAGRA MR. 2010. Homeotic effects, somitogenesis and the evolution of vertebral numbers in recent and fossil amniotes. P Natl Acad Sci USA 107(5): 2118-2123.

NAISH D & WITTON MP. 2017. Neck biomechanics indicate that giant Transylvanian azhdarchid pterosaurs were short-necked arch predators. PeerJ 5: e2908.

NESOV LA. 1984. Pterosaurs and birds of the Late Cretaceous of Central Asia. Palaontologische Zeitschrift 1: 47-57.

NICHOLLS EL & RUSSELL AP. 1985. Structure and function of the pectoral girdle and forelimb of *Struthiomimus altus* (Theropoda: Ornithomimidae). Palaeontology 28: 643-677.

PADIAN K. 2008. The Early Jurassic pterosaur *Dorygnathus bathensis* (Theodori, 1830). Spec Pap Palaeontol 80: 1-64.

PADIAN K, CUNNINGHAM JR, LANGSTON-JR W & CONWAY J. 2021. Functional morphology of *Quetzalcoatlus* Lawson 1975 (Pterodactyloidea: Azhdarchoidea). J Vertebr Paleontol 41: 218-251.

PÊGAS RV, COSTA FR & KELLNER AWA. 2020. Reconstruction of the adductor chamber and predicted bite force in pterodactyloids (Pterosauria). Zoo J Linn Soc 193: 602-635.

PHALAN B, PHILLIPS RA, SILK JRD, AFANASYEV V, FUKUDA A, FOX J, CATRY P, HIGUCHI H & CROXALL JP. 2007. Foraging behaviour of four albatross species by night and day. Mar Ecol Prog Ser 340: 271-286.

PINHEIRO FL, FORTIER DC, SCHULTZ CL, DE ANDRADE JAFG & BANTIM RAM. 2011. New information on the pterosaur *Tupandactylus imperator*, with comments on the relationships of Tapejaridae. Acta Palaeontol Pol 56(3): 567-580

PINHEIRO FL & RODRIGUES T. 2017. *Anhanguera* taxonomy revisited: is our understanding of Santana Group pterosaur diversity biased by poor biological and stratigraphic control? PeerJ 5: e3285.

PONSETI IV. 1995. Differences in *ligamenta flava* among some mammals. Lowa Orthop 15: 141-146.

PORRO LB, HOLLIDAY CM, ANAPOL F, ONTIVEROS LC, ONTIVEROS LT & ROSS CF. 2011. Free body analysis, beam mechanics, and finite elements modeling of the mandible of *Alligator mississippiensis*. J Morphol 272: 910-937.

PRIETO IR. 1998. Morfología funcional y hábitos alimentarios de *Quetzalcoatlus* (Pterosauria). Coloquios de Paleontologia 49: 129-144.

REDFORD KH & PETERS G. 1986. Notes on the biology and song of the red-legged seriema (*Cariama cristata*). J Field Ornithol 57(4): 261-353.

SCHREIBER EA & BURGER J. 2001. Biology of Marine Birds, Boca Raton: CRC Press, 740 p.

SEIDEL R. 1978. The somatic musculature of the cervical and occipital regions of *Alligator mississippiensis*. PhD dissertation, City University of New York.

SELBIE WB, THOMSON DB & RICHMOND FJR. 1993. Sagittal-plane mobility of the cat cervical spine. J Biomech 26(8): 917-927.

SICK H. 1997. Ornitologia Brasileira, 1st ed., Rio de Janeiro: Editora Nova Fronteira, 912 p.

SNIVELY E, COTTON JR, RIDGELY R & WITMER LM. 2013. Multibody dynamics model of head and neck function in allosaurs (Dinosauria, Theropoda). Palaeontol Electron 16(2): 10.26879/338.

SNIVELY E & RUSSELL AP. 2007. Functional morphology of neck musculature in the Tyrannosauridae (Dinosauria, Theropoda) as determined via a hierarchical inferential approach. Zool J Linn Soc-Lond 151: 759-808.

TAMBUSSI CP, DE MENDOZA R, DEGRANGE FJ & PICASSO MB. 2012. Flexibility along the Neck of the Neogene Terror Bird *Andalgalornis steulleti* (Aves Phorusrhacidae). PLoS ONE 7(5): e37701.

TAYLOR MP, WEDEL MJ & NAISH D. 2009. Head and neck posture in sauropod dinosaurs inferred from extant animals. Acta Palaeontol Pol 54(2): 213-220.

TERRAY L, PLATEAU O, ABOURACHID A, BÖHMER C, DELAPRÉ A, DE LA BERNARDIE X & CORNETTE R. 2020. Modularity of the neck in birds (Aves). Evol Biol 47: 97-110.

TSUIHIJI T. 2004. The ligament system in the neck of *Rhea americana* and its implication for the bifurcated neural spines of sauropod dinosaurs. J Vertebr Paleontol 24(1): 165-172.

TSUIHIJI T. 2005. Homologies of the *transversospinalis* muscles in the anterior presacral region of Sauria (crown Diapsida). J Morphol 263: 151-178.

TSUIHIJI T. 2007. Homologies of the *longissimus*, *iliocostalis*, and hypaxial muscles in the anterior presacral region of extant diapsida. J Morphol 268: 986-1020.

TÜTKEN T & HONE DWE. 2010. The ecology of pterosaurs based on carbon and oxygen isotope analysis. Acta Geoscientica Sinica 31: 65-67.

VANDEN-BERGE JC, ZWEERS GA. 1993. Myologia In: Baumel JJ, King AS, Breazile JC, Evans HE & Vanden Berge JC (Eds), Handbook of avian anatomy: *Nomina anatomica avium*, Cambridge: Nuttal Ornihtological Club, p. 189-247.

VELDMEIJER AJ, MEIJER HJM & SIGNORE M. 2009. Description of pterosaurian (Pterodactyloidea: Anhangueridae, *Brasileodactylus*) remains from the Lower Cretaceous of Brazil. Deinsea 13: 9-40.

VELDMEIJER AJ, SIGNORE M & BUCCI E. 2007. Predator-prey interaction of Brazilian Cretaceous toothed pterosaurs: a case example. In: Elewa AMT (Ed), Predation in organisms: a distinct phenomenon. Berlin, Heidelberg: Springer, p. 295-308.

VELDMEIJER AJ, WITTON MP & NIEUWLAND I. 2012. Pterosaurs: Flying contemporaries of the dinosaurs, Leiden: Sidestone Press, 133 p.

VIDAL D, MOCHO P, PÁRAMO A, SANZ JL & ORTEGA F. 2020. Ontogenetic similarities between giraffe and sauropod neck osteological mobility. PLoS ONE 15(1): e0227537.

VIDAL PP, GRAF W & BERTHOZ A. 1986. The orientation of the cervical vertebral column in unrestrained awake animals. Exp Brain Res 61: 549-559.

VILA NOVA BC, SAYÃO JM, LANGER MC & KELLNER AWA. 2015. Comments on the cervical vertebrae of the Tapejaridae (Pterosauria, Pterodactyloidea) with description of new specimens. Hist Biol 27: 770-780.

WANG X, KELLNER AWA, JIANG S & CHENG X. 2012. New toothed flying reptile from Asia: close similarities between early Cretaceous pterosaur faunas from China and Brazil. Naturwissenschaften 99: 249-257.

WEIMERSKIRCH H, CHEREL Y, DELORD K, JAEGER A, PATRICK SC & RIOTTE-LAMBERT L. 2013. Lifetime foraging patterns of the wandering albatross: Life on the move! J Exp Mar Biol Ecol 450: 68-78.

WELLNHOFER P. 1975. Die Rhamphorhynchoidea (Pterosauria) der Oberjura-Plattenkalke Süddeutschlands. I: Allgemeine Skelettmorphologie. Paleontogr Abt A 148: 132-186.

WELLNHOFER P. 1991a. The illustrated encyclopedia of prehistoric flying reptiles. London: Salamander Books, 192 p.

WELLNHOFER P. 1991b. Weitere Pterosaurierfunde aus der Santana-Formation (Apt) der Chapada do Araripe, Brasilien. Paleontogr Abt A 215: 43-101.

WILLIAMS CJ, PANI M, BUCCHI A, SMITH RE, KAO A, KEEBLE W, IBRAHIM N & MARTILL DM. 2021. Helically arranged cross struts in azhdarchid pterosaur cervical vertebrae and their biomechanical implications. iScience 24: 102338.

WINTRICH T, JONAS R, WILKE HJ, SCHMITZ L & SANDER PM. 2019. Neck mobility in the Jurassic plesiosaur *Cryptoclidus eurymerus*: finite element analysis as a new approach to understanding the cervical skeleton in fossil vertebrates. PeerJ 7: e7658.

WITMER LM. 1995. The Extant Phylogenetic Bracket and the importance of reconstructing soft tissues in fossils. In: Thomason JJ (Ed), Functional morphology in vertebrate palaeontology, Cambridge: Cambridge University Press, p. 19-33.

WITMER LM, CHATTERJEE S, FRANZOSA J & ROWE T. 2003. Neuroanatomy of flying reptiles and implications for flight, posture and behavior. Nature 425: 950-953.

WITTON MP & HABIB MB. 2010. On the size and flight diversity of giant pterosaurs, the use of birds as pterosaur analogues comments on pterosaur flightlessness. PLoS ONE 5: e13982.

WITTON MP & NAISH D. 2008. A reappraisal of azhdarchid pterosaur functional morphology and paleoecology. PLoS ONE 3: e2271.

WITTON MP & NAISH D. 2015. Azhdarchid pterosaurs: water-trawling pelican mimics of terrestrial stalkers? Acta Palaeontol Pol 60: 651-660.

ZUSI RL. 1962. Structural adaptations of the head and neck in the Black Skimmer, *Rhynchops nigra* Linnaeus. Publ Nuttal Ornithological Club 3: 1-153.

ZWEERS GA, BOUT R & HEIDWEILLER J. 1994. Motor organization of avian head-neck system. In: David M & Green P (Eds),

Perception and motor control in birds, Berlin: Springer-Verlag, p. 201-221.

ZWEERS GA, VANDEN-BERGE JC & KOPPENDRAIER R. 1987. Avian cranio-cervical systems. Part I: Anatomy of the cervical column in the chicken (*Gallus gallus*). Acta Morphol Neer Sc 25: 131-155.

SUPPLEMENTARY MATERIAL

Tables SI, SII and SIII.

How to cite

BUCHMANN R & RODRIGUES T. 2025. Flesh and bone: The musculature and cervical movements of pterosaurs. An Acad Bras Cienc 97: e20240478. DOI 10.1590/0001-3765202520240478.

Manuscript received on May 9, 2024;
accepted for publication on December 2, 2024

RICHARD BUCHMANN[1,2]
https://orcid.org/0000-0003-4428-9224

TAISSA RODRIGUES[1,2]
https://orcid.org/0000-0001-7918-1358

[1]Universidade Federal do Espírito Santo, Departamento de Ciências Biológicas, Laboratório de Paleontologia, Avenida Fernando Ferrari, 514, 29075-910 Vitória, ES, Brazil

[2]Universidade Federal do Espírito Santo, Programa de Pós-graduação em Ciências Biológicas, Avenida Fernando Ferrari, 514, 29075-910 Vitória, ES, Brazil

Correspondence to: **Richard Buchmann**
E-mail: richardbuchmann@gmail.com

Author contributions

RICHARD BUCHMANN: Conceptualization; investigation; methodology; validation; visualization; writing – review and editing; writing – original draft; formal analysis; project administration; resources; data curation; software. TAISSA RODRIGUES: Conceptualization; funding acquisition; writing – review and editing; supervision; project administration; resources.